An MBO scheme for minimizing the graph Ohta-Kawasaki functional: supplementary materials

Yves van Gennip

University of Nottingham

May 14, 2018

In these Supplementary Materials, we indicate references to the main paper by the prefix "M".

1 The continuum Ohta-Kawasaki model

In this section we give a brief introduction to the continuum Ohta-Kawasaki model which was introduced into the physics/chemistry literature to describe diblock copolymer melts. This model has been studied intensively in recent decades and this section is not aiming to be exhaustive or even extensive. For a sample of mathematical papers on this topic, see for example [RW00, RW02, RW03a, RW03b, CR03, CR05, CS06, vGP08, vGP09, CPW09, GC09, Le10, PV10, CP10, CP11, CMW11, vGP11, Cho12, BPR14, RW14, RW17, Gla17].

The continuum Ohta-Kawasaki functional [OK86, KOK88] comes in a diffuse interface form, $F_\varepsilon : H^{-1}(\Omega;\mathbb{R}) \to \mathbb{R}$,

$$\mathcal{F}_\varepsilon(u) := \frac{1}{2}\int_\Omega |\nabla u|^2 + \frac{1}{\varepsilon}\int_\Omega W(u) + \frac{\gamma}{2}\left\|u - \frac{1}{|\Omega|}\int_\Omega u\right\|^2_{H^{-1}(\Omega)},$$

and a sharp interface form, $F_0 : BV(\Omega;\{-1,1\}) \to \mathbb{R}$,

$$\mathcal{F}_\varepsilon(u) := \sigma\int_\Omega |\nabla u| + \frac{\gamma}{2}\left\|u - \frac{1}{|\Omega|}\int_\Omega u\right\|^2_{H^{-1}(\Omega)}.$$

Here $\Omega \subset \mathbb{R}^n$ is an open, bounded set, ε, γ, and σ are positive parameters, and W denotes a nonnegative double well potential with equal depth wells, for example the double well potential in (M30) with wells at $x \in \{0,1\}$. The total variation [Giu84] is defined as

$$\int_\Omega |\nabla u| := \sup\left\{\int_\Omega u, \operatorname{div} v : \ v \in C_0^\infty(\Omega;\mathbb{R}^n),\ \forall x \in \Omega\, |v(x)| \le q\right\},$$

and the negative Sobolev H^{-1} norm as

$$\left\|u - \frac{1}{|\Omega|}\int_\Omega u\right\|^2_{H^{-1}(\Omega)} := \int_\Omega |\nabla\varphi|^2,$$

where $\varphi \in H^1(\Omega)$ solves $\Delta\varphi = u - \frac{1}{|\Omega|}\int_\Omega u$ with appropriate boundary conditions (which can vary depending on the context). The diffuse interface functional $\mathcal{F}_\varepsilon$ is an approximation of the sharp interface functional $\mathcal{F}_0$ in the sense of Γ-convergence: any sequence of functionals $\mathcal{F}_\varepsilon$ Γ-converges to $\mathcal{F}_0$ when $\varepsilon \to 0$ in the $L^1(\Omega)$ topology [MM77, Mod87a, Mod87b]. Note in particular that $\mathcal{F}_0$ is defined on binary functions that take values ± 1 only. For such functions $\frac{1}{2}\int_\Omega |\nabla u|$ computes the length of the (reduced) boundary [AFP00, Definition 3.54] between the set where $u = -1$ and the set where $u = 1$. In this limit, the surface tension parameter $\sigma > 0$ is determined by the specific choice of W, but its precise value is not of importance here.

When $\mathcal{F}_0$ (or $\mathcal{F}_\varepsilon$) is minimized under a mass constraint $\frac{1}{|\Omega|}\int_\Omega u = M$, the boundary minimizing effect of the total variation term competes with the mixing preference of the H^{-1} norm, which leads to pattern formation on a scale determined by the parameter γ, which controls the relative influence of both terms. The mass parameter M has large impact on the type of patterns that appear. When M is close to -1 or close to 1, such that one phase is much more prevalent than the other, small droplets of the minority phase will form in a background formed by the majority phase; when $M \approx 0$ a lamellar phase forms; see for example [BF99, Figure 3] for a simplified theoretical sketch of some of the expected patterns in a physical diblock copolymer system. A goal in the mathematical literature has been to prove the existence of various patterns that appear as minimizers and study their stability, see for example [RW00, RW02, RW03a, RW03b, RW14, RW17]. Extensions of the model, for example including a third phase either through triblock copolymers or through adding a homopolymer, have also been considered, for example in [UD05, vG08, vGP08, vGP09].

2 Random walk interpretation of the Green's function

For more information about the general concepts discussed in this section, see e.g. [Chu97, DS00, Sig].

Consider a discrete time random walk on the graph $G = (V, E, \omega) \in \mathcal{G}$, with transition probabilities, for all $i, j \in V$, $p_{ij} := d_i^{-1}\omega_{ij}$, i.e. the probability of moving from vertex i to vertex j in one time step is $d_i^{-1}\omega_{ij}$. Note that $\sum_{j\in V} p_{ij} = 1$.

For all $i \in V$, let T_i be the earliest time step at which the random walk is at node i. By convention, let the random walk start at time 0. Now (remembering that $|V| \geq 2$) fix two different vertices $a, b \in V$ and define $h \in \mathcal{V}$, by, for all $i \in V$, $h_i := P[T_a < T_b | T_i = 0]$, i.e. h_i is the probability the random walk starting from node i reaches a before it reaches b. Clearly $h_a = 1 \quad \text{and} \quad h_b = 0$. Moreover, since the walk at each time step is independent, we have, for $i \in V \setminus \{a, b\}$ (and for any $r \in [0, 1]$), $h_i = \sum_{j\in V} p_{ij} h_j$ or, equivalently, $(\Delta h)_i = 0$. If, for all $i \in V$, $\tilde{h}_i := P[T_b < T_a | T_i = 0]$ (note that the roles of a and b are exchanged, compared to h) and $h^+ := h + \tilde{h}$, then $\Delta h^+ = 0$ on $V \setminus \{a, b\}$ and $h_a^+ = h_b^+ = 1$, hence $h_i^+ = 1$ for all $i \in V$, as expected (the probability that the random walk either reaches a before b, or b before a, is 1).

Conversely to the computation for h above, if $v \in \mathcal{V}$ solves

$$\begin{cases} (\Delta v)_i = 0, & \text{if } i \in V \setminus \{a, b\}, \\ v_a = c, & \text{for some } c \in \mathbb{R}, \\ v_b = 0, \end{cases}$$

then, for each $i \in V$, v_i is the expected payoff value in a game consisting of a random walk starting at $i \in V$, with payoff equal to c if the walk reaches a before b and zero otherwise. (Since the same equation is satisfied by the voltage function on an electric network with voltage c applied to node a and voltage 0 to node b, such a v can also be interpreted as voltage on an electric network [DS00].)

Consider now the Green's function for the Poisson equation satisfying (M23) with (M24) and (M25), for $j = a \in V$ and $k = b \in V$, then,

$$\begin{cases} (\Delta G^a)_i = 0, & \text{if } i \in V \setminus \{a, b\}, \\ G_a^a = \frac{1}{\text{vol}(V)} \left(\nu_a^{V\setminus\{b\}} + \nu_b^{V\setminus\{a\}} \right), \\ G_b^a = 0, \end{cases}$$

where we used (M27) for the second line. Hence G_i^a is the expected payoff of the game described above with the walk starting at $i \in V$ and $c = c_{ab} := \frac{1}{\text{vol}(V)} \left(\nu_a^{V\setminus\{b\}} + \nu_b^{V\setminus\{a\}} \right) > 0$. Positivity of c_{ab} follows from positivity of the equilibrium measures $\nu_a^{V\setminus\{b\}}$ and $\nu_b^{V\setminus\{a\}}$ (Definition M3.3). Note that c_{ab} implicitly depends on r.

3 Γ-convergence of F_ε

In this section we prove that the diffuse interface graph Ohta-Kawasaki functionals from (M31) converge to the limit functional F_0 (M32) in the sense of Γ-convergence. The upper bound and lower bound

properties of Theorem M5.10 (or Theorem M5.13) are the two defining conditions of Γ-convergence. We refer the reader to [DM93, Bra02] for a detailed definition and important properties of Γ-convergence.

Note that in the results below, we do not specify the topology under which the convergence of sequences in $\mathcal{V}$ are considered. We can use $\|\cdot\|_{\mathcal{V}}$, but any other norm based topology will be equivalent in this finite dimensional setting.

We remind the reader that $\overline{\mathbb{R}}$ denotes the extended real line $\mathbb{R} \cup \{-\infty + \infty\}$.

Lemma 3.1. *Let $G = (V, E, \omega) \in \mathcal{G}$ and let $\{\varepsilon_k\}_{k\in\mathbb{N}}$ be a sequence such that, for all $k \in \mathbb{N}$, $\varepsilon_k > 0$ and $\varepsilon_k \to 0$ as $k \to \infty$. For each $k \in \mathbb{N}$, define $F_{\varepsilon_k} : \mathcal{V} \to \overline{\mathbb{R}}$ by the expression in (M31) and let $\hat{F}_0 : \mathcal{V} \to \overline{\mathbb{R}}$ be defined as*

$$\hat{F}_0(u) := \begin{cases} F_0(u), & \text{if } u \in \mathcal{V}^b, \\ +\infty, & \text{otherwise,} \end{cases}$$

where F_0 is as in (M32). Then $\{F_{\varepsilon_k}\}_{k\in\mathbb{N}}$ Γ-converges to $\hat{F}_0$ as $k \to \infty$.

Moreover, if $\{u_k\}_{k\in\mathbb{N}} \subset \mathcal{V}$ and there exists a $C > 0$ such that, for all $k \in \mathbb{N}$, $F_{\varepsilon_k}(u_k) < C$, then there is a subsequence $\{u_{k_l}\}_{l\in\mathbb{N}} \subset \{u_k\}_{k\in\mathbb{N}}$ and a $u \in \mathcal{V}^b$ such that $u_{n_k} \to u$ as $k \to \infty$.

Proof. A proof of the Γ-convergence of the terms $\frac{1}{2}\|\nabla u\|^2_{\mathcal{E}} + \frac{1}{\varepsilon_n}\sum_{i\in V} W(u_i)$ in F_{ε_n} is given in [vGB12, Section 3.1]. Since Γ-convergence is stable under continuous perturbations [DM93, Proposition 6.21] and both the map $u \mapsto u - \mathcal{A}(u)$ and the H^{-1} norm are continuous, the Γ-convergence statement follows. The compactness result in the second part of the lemma's statement follows directly from [vGB12, Section 3.1]. □

Lemma 3.2 (Γ-convergence with a mass constraint)**.** *Let $G = (V, E, \omega) \in \mathcal{G}$ and let $\{\varepsilon_k\}_{k\in\mathbb{N}}$ be a sequence such that, for all $k \in \mathbb{N}$, $\varepsilon_k > 0$ and $\varepsilon_k \to 0$ as $k \to \infty$. Let $M \in \mathfrak{M}$, where $\mathfrak{M}$ is the set of admissible masses as in (M11) in the main paper. For each $k \in \mathbb{N}$, define $\breve{F}_{\varepsilon_k} : \mathcal{V}_M \to \overline{\mathbb{R}}$ by $\breve{F}_{\varepsilon_k} := F_{\varepsilon_k}\big|_{\mathcal{V}_M}$, where F_{ε_k} is as in (M31), and let $\breve{F}_0 : \mathcal{V}_M \to \overline{\mathbb{R}}$ be defined as $\breve{F}_0 := \hat{F}_0\big|_{\mathcal{V}_M}$, where $\hat{F}_0$ is as in Lemma 3.1. Then $\{\breve{F}_{\varepsilon_k}\}_{k\in\mathbb{N}}$ Γ-converges to $\breve{F}_0$ as $k \to \infty$.*

Moreover, if $\{u_k\}_{k\in\mathbb{N}} \subset \mathcal{V}$ and there exists a $C > 0$ such that, for all $k \in \mathbb{N}$, $\breve{F}_{\varepsilon_k}(u_k) < C$, then there is a subsequence $\{u_{k_l}\}_{l\in\mathbb{N}} \subset \{u_k\}_{k\in\mathbb{N}}$ and a $u \in \mathcal{V}_0$ such that $u_{k_l} \to u$ as $l \to \infty$.

Proof. The only difference between this result and that of Lemma 3.1, is that now the definitions of $\breve{F}_{\varepsilon_n}$ and $\breve{F}_0$ incorporate a mass constraint in their domains. Analogously to the argument in [vGB12, Section 3.2], we see that by continuity of $u \mapsto \mathcal{M}(u)$, the proof of the lower bound in the Γ-convergence proof and the proof of the compactness result remain unchanged from the case of Lemma 3.1. For the proof of the upper bound, we note, as in [vGB12, Section 3.2], that the recovery sequence used in this proof will satisfy the same mass constraint as its limit. □

4 Gradient flows of F_ε

Let $u, v \in \mathcal{V}$ and $s \in \mathbb{R}$. Let $\varphi, \psi \in \mathcal{V}$ satisfy $\Delta\varphi = u - \mathcal{A}(u)$ and $\Delta\psi = v - \mathcal{A}(v)$, respectively, then $\Delta(\varphi + s\psi) = u + sv - \mathcal{A}(u + sv)$. Hence, using (M2), we find

$$\begin{aligned} \frac{d}{ds}\|u + sv - \mathcal{A}(u + sv)\|^2_{H^{-1}}\Big|_{s=0} &= \frac{d}{ds}\langle u - \mathcal{A}(u) + sv - s\mathcal{A}(v), \varphi + s\psi\rangle_{\mathcal{V}}\Big|_{s=0} \\ &= \langle u - \mathcal{A}(u), \psi\rangle_{\mathcal{V}} + \langle v - \mathcal{A}(v), \varphi\rangle_{\mathcal{V}} \\ &= \langle \Delta\varphi, \psi\rangle_{\mathcal{V}} + \langle v - \mathcal{A}(v), \varphi\rangle_{\mathcal{V}} = 2\langle v - \mathcal{A}(v), \varphi\rangle_{\mathcal{V}}. \end{aligned}$$

We note that $\langle \mathcal{A}(v), \varphi\rangle_{\mathcal{V}} = \frac{1}{\mathrm{vol}(V)}\sum_{i,j\in V} d_i^r v_i d_j^r \varphi_j = \left\langle v, \left(\frac{1}{\mathrm{vol}(V)}\sum_{j\in V} d_j^r \varphi_j\right)\chi_V \right\rangle_{\mathcal{V}} = \langle v, \mathcal{A}(\varphi)\rangle_{\mathcal{V}}$, hence

$$\frac{d}{ds}\|u + sv - \mathcal{A}(u + sv)\|^2_{H^{-1}}\Big|_{s=0} = 2\langle v, \varphi - \mathcal{A}(\varphi)\rangle_{\mathcal{V}}.$$

Using the gradient of the first terms in F_ε as computed in [vGGOB14, Section 5], we deduce that

$$\frac{d}{ds}F_\varepsilon(u + sv)\Big|_{s=0} = \left\langle \Delta u + \frac{1}{\varepsilon}d^{-r}W'(u) + \gamma\big(\varphi - \mathcal{A}(\varphi)_i\big), v\right\rangle_{\mathcal{V}},$$

where $d^{-r}W'(u)$ is to be interpreted as the function in $\mathcal{V}$ defined by $(d^{-r}W'(u))_i := d_i^{-r}W'(u_i)$, for all $i \in V$. Using (M28) we can also write

$$\frac{d}{ds}F_\varepsilon(u+sv)\Big|_{s=0} = \big\langle \Delta\big\{\Delta u + \frac{1}{\varepsilon}d^{-r}W'(u) + \gamma\big(\varphi - \mathcal{A}(\varphi)\big)\big\}, v\big\rangle_{H^{-1}}.$$

We note that, as expected, the freedom to add an arbitrary constant to φ has no influence on the final result.

Hence, the $\mathcal{V}$ gradient flow is the *Allen-Cahn type system of equations*

$$\frac{d}{dt}u_i = -(\Delta u)_i - \frac{1}{\varepsilon}d_i^{-r}W'(u_i) - \gamma(\varphi_i - \mathcal{A}(\varphi)_i), \quad \text{for } i \in V, \tag{1}$$

while the H^{-1} gradient flow leads to the *Cahn-Hillard type system of equations*

$$\frac{d}{dt}u_i = -(\Delta(\Delta u))_i - \frac{1}{\varepsilon}\Delta(d^{-r}W'(u))_i - \gamma(u_i - \mathcal{A}(u)_i), \quad \text{for } i \in V. \tag{2}$$

The functions u and φ are in $\mathcal{V}_\infty$ (which is defined near the start of Section M5.1 in the main paper) as is usual for gradient flows[1]. We did not write the explicit dependence on t here.

Since we are interested in minimising F_ε over the set $\mathcal{V}_M$ of node functions with mass M, as defined in (M7), we need to ensure that the mass of u does not change along the gradient flow. Because the right hand side of (2) is of the form $\Delta f(u(t))$, with $f : \mathcal{V} \to \mathcal{V}$ determined by (2), for any solution of the H^{-1} gradient flow above we have, by (M4), $\frac{d}{dt}\mathcal{M}(u(t)) = \mathcal{M}\left(\frac{du(t)}{dt}\right) = \mathcal{M}\big(\Delta f(u(t))\big) = 0$.

For the $\mathcal{V}$ gradient flow mass conservation is not guaranteed and we need to introduce a Langrange multiplier $\mu : [0,\infty) \to \mathbb{R}$ in the equation: $\frac{d}{dt}u_i = -(\Delta u)_i - \frac{1}{\varepsilon}d_i^{-r}W'(u_i) - \gamma\big(\varphi_i - \mathcal{A}(\varphi)\big) - \mu$, such that

$$0 = \frac{d}{dt}\mathcal{M}(u) = -\mathcal{M}\big(\Delta u + \gamma(\varphi_i - \mathcal{A}(\varphi))\big) - \frac{1}{\varepsilon}\sum_{i\in V}W'(u_i) + \mu\mathrm{vol}\,(V) = -\frac{1}{\varepsilon}\sum_{i\in V}W'(u_i) + \mu\mathrm{vol}\,(V)\,.$$

Hence $\frac{d}{dt}\mathcal{M}(u) = 0$ if and only if $\mu = \dfrac{1}{\varepsilon\,\mathrm{vol}\,(V)}\displaystyle\sum_{i\in V}W'(u_i)$. Therefore the mass constrained Allen-Cahn equation becomes

$$\begin{aligned}\frac{d}{dt}u_i &= -(\Delta u)_i - \frac{1}{\varepsilon}\left(d_i^{-r}W'(u_i) - (\mathrm{vol}\,(V))^{-1}\sum_{j\in V}W'(u_j)\right) - \gamma\big(\varphi_i - \mathcal{A}(\varphi)\big)\\ &= -(\Delta u)_i - \frac{1}{\varepsilon}\big(d_i^{-r}W'(u_i) - \mathcal{A}\left(d^{-r}W'(u)\right)_i\big) - \gamma\big(\varphi_i - \mathcal{A}(\varphi)\big).\end{aligned} \tag{3}$$

5 Further details about M(OKMBO)

5.1 Green's functions and equilibrium measures

The following remark and lemma address the relationship between solutions of (M29) and (M45).

Remark 5.1. Note that we cannot always find a $k \in V$ such that the solution to (M29) is also a solution to (M45). In other words, the solution to (M45) with $\mathcal{M}(\varphi) = 0$ may have nonzero value at every node in V. We could keep definition (M29) for φ, instead of (M45), but then we would need to replace the term $-\gamma\varphi$ in (M47) (with (M46)) by $-\gamma(\varphi - \mathcal{A}(\varphi))$. For simplicity we choose the formulation as laid out in (M47) with (M45), but this has as consequence that φ from (M45) cannot necessarily always be obtained via the Green's function approach outlined in (M19), (M27). In general such φ will have the form, for all $i \in V$, $\varphi_i := \sum_{j\in S} d_j^r G_{ij}(u_j - \mathcal{A}(u)) + c$, where G is as in (M27) and c is a suitably chosen constant such that $\mathcal{M}(\varphi) = 0$. Of course, as remarked before, the value of c will not influence the value of $\|u - \mathcal{A}(u)\|_{H^{-1}}$.

Lemma 5.2 below gives a sufficient condition for c to be zero.

The next lemma uses the equilibrium measures from Definition M3.3.

[1] Note that Peano's existence theorem [Hal09, Theorem 1.1] guarantees existence of a continuously-differentiable-in-t solution u of equations (1) (2), and (3), because in each of these the right hand side can be written as Ou, where O is a continuous operator from $\mathcal{V}$ to $\mathcal{V}$. Continuity of O follows from continuity of W' and (M55).

Lemma 5.2. *Let $k \in V$ and let φ solve (M29). If there exists an $l \in V$ such that, for all $j \in V$,*

$$\nu_l^{V\setminus\{k\}} - \nu_l^{V\setminus\{j\}} = \frac{1}{\mathrm{vol}\,(V)} \sum_{i\in V} d_i^r \left(\nu_i^{V\setminus\{k\}} - \nu_i^{V\setminus\{j\}}\right),$$

then $\tilde{\varphi} := \varphi - \varphi_l$ satisfies both (M45) and $\begin{cases} \Delta\tilde{\varphi} = u - \mathcal{A}(u), \\ \tilde{\varphi}_l = 0. \end{cases}$

Proof. Clearly $\tilde{\varphi}_l = 0$ and, since φ satisfies (M29), $\Delta\tilde{\varphi} = u - \mathcal{A}(u)$. Let G be the Green's function from (M27). If the conditions from the lemma hold, then, for all $j \in V$,

$$\begin{aligned} G_{lj} &= \frac{1}{\mathrm{vol}\,(V)} \left(\nu_l^{V\setminus\{k\}} + \nu_k^{V\setminus\{j\}} - \nu_l^{V\setminus\{j\}}\right) = \frac{1}{\mathrm{vol}\,(V)} \left[\nu_k^{V\setminus\{j\}} + \frac{1}{\mathrm{vol}\,(V)} \sum_{i\in V} d_i^r \left(\nu_i^{V\setminus\{k\}} - \nu_i^{V\setminus\{j\}}\right)\right] \\ &= \frac{1}{\mathrm{vol}\,(V)^2} \sum_{i\in V} d_i^r \left(\nu_i^{V\setminus\{k\}} + \nu_k^{V\setminus\{j\}} - \nu_i^{V\setminus\{j\}}\right) (\chi_V)_i = \frac{1}{\mathrm{vol}\,(V)} \langle G^j, \chi_V\rangle_{\mathcal{V}} = \mathcal{A}(G^j). \end{aligned}$$

Therefore[2], $\varphi_l = \langle G_{l\bullet}, u - \mathcal{A}(u)\rangle_{\mathcal{V}} = \langle \mathcal{A}(G^\bullet), u - \mathcal{A}(u)\rangle_{\mathcal{V}}$. Moreover,

$$\mathcal{M}(\varphi) = \sum_{i\in V} \varphi_i d_i^r = \sum_{i,j\in V} G_{ij}(u_j - \mathcal{A}(u)) d_i^r d_j^r = \sum_{j\in V} \mathcal{M}(G_{\bullet j})(u_j - \mathcal{A}(u)) d_j^r = \langle \mathcal{M}(G^\bullet), u - \mathcal{A}(u)\rangle_{\mathcal{V}}.$$

Hence we conclude that $\varphi_l = \mathcal{A}(\varphi)$ and thus $\varphi - \varphi_l$ satisfies (M45). □

Remark 5.3. The symmetry property of the Green's function for the Dirichlet equation in Lemma M3.16 from the main paper allows us to note that, if we write the equilibrium measure ν^S which solves the Dirichlet problem in (M12) in terms of the Green's function for the Dirichlet equation from (M26), using (M18), we find the consistent relationship, for $i \in S$,

$$\nu_i^S = \sum_{j\in S} d_j^r G_{ij} (\chi_S)_j = \sum_{j\in V} d_j^r G_{ji} (\chi_S)_j = \sum_{j\in V} d_j^r \nu_i^S \frac{\nu_j^S - \nu_j^{S\setminus\{i\}}}{\mathcal{M}(\nu^S) - \mathcal{M}(\nu^{S\setminus\{i\}})} (\chi_S)_j = \nu_i^S.$$

For the last equality, we used that, by property M3 from Lemma M3.2, $\nu_j^S - \nu_j^{S\setminus\{i\}} = 0$ if $j \in V \setminus S$, hence the factor $(\chi_S)_j$ can be replaced by $(\chi_V)_j$ without changing the value of the summation.

Remark 5.4. Combining property M3 from Lemma M3.2 regarding the support of the equilibrium measure with (M26), we see that we could consistently extend the Green's function for the Dirichlet equation to a function $V \times V$, by setting $G_{ij} = 0$ for $j \in V \setminus S$. In that case (M18) takes the same form as in the Poisson case, (M19). The defining properties (M21) will still hold, as will the symmetry property from Lemma M3.16 (now for all $i, j \in V$).

In this paper (both the main paper and these Supplementary Materials) we stick to the original domain $V \times S$ for the Green's function for the Dirichlet equation.

5.2 The spectrum of L

In this section we will have a closer look at the spectrum of the operator L from (M46).

Remark 5.5. Note that in the notation of Lemma M5.8, the eigenvalues Λ_m are not necessarily labelled in non-decreasing order. In fact, the function $f : (0,\infty) \to (0,\infty), x \mapsto x + \frac{\gamma}{x}$ achieves its unique minimum on $(0,\infty)$ at $x = \sqrt{\gamma}$ and is decreasing for $0 < x < \sqrt{\gamma}$ and increasing for $x > \sqrt{\gamma}$. Hence, if $\lambda_{n-1} \leq \sqrt{\gamma}$, then the Λ_m are in non-increasing order, except for Λ_0, which is always the smallest eigenvalue. On the other hand, if $\lambda_1 \geq \sqrt{\gamma}$, then the Λ_m are in non-decreasing order. If neither of these conditions on λ_1 or λ_{n-1} is met, the order is not guaranteed to be monotone.

[2] The index $\bullet$ in $G_{l\bullet}$ and $\mathcal{A}(G^\bullet)$ indicates the index over which is summed in the inner products; thus in the second inner product the summation in the mass $\mathcal{M}(G^j)$ is over the lower index of G_i^j (for fixed j) and the summation in the inner product is over the upper index.

Definition 5.6. *Let $G = (V, E, \omega) \in \mathcal{G}$, $\gamma \geq 0$, and let Λ_m ($m \in \{0, \dots, n-1\}$) be the eigenvalues of L as in (M56). The smallest nonzero eigenvalue of L is $\Lambda_- := \min_{1 \leq m \leq n-1} \Lambda_m$, and the largest eigenvalue (or spectral radius) of L is $\Lambda_+ := \max_{0 \leq m \leq n-1} |\Lambda_m|$.*

Lemma 5.7 characterizes the smallest nonzero eigenvalue and the largest eigenvalue of L. These eigenvalues will be of importance in Section 5.3.

Lemma 5.7. *Let $G = (V, E, \omega) \in \mathcal{G}$ and let λ_m ($m \in \{0, \dots, n-1\}$) be the eigenvalues of Δ as in (M35). If $\lambda_1 \leq \sqrt{\gamma} \leq \lambda_{n-1}$, we define $\lambda_* := \max\{\lambda_m : 1 \leq m \leq n-1 \text{ and } \lambda_m \leq \sqrt{\gamma}\}$ and $\gamma^* := \min\{\lambda_m : 1 \leq m \leq n-1 \text{ and } \lambda_m \geq \sqrt{\gamma}\}$. Then the value of Λ_- from Definition 5.6 is given by*

$$\Lambda_- = \begin{cases} \lambda_1 + \frac{\gamma}{\lambda_1}, & \text{if } \lambda_1 > \sqrt{\gamma}, \\ \lambda_* + \frac{\gamma}{\lambda_*}, & \text{if } \lambda_1 \leq \sqrt{\gamma} < \sqrt{\lambda_* \lambda^*} \leq \lambda_{n-1}, \\ \lambda^* + \frac{\gamma}{\lambda^*}, & \text{if } \lambda_1 \leq \sqrt{\lambda_* \lambda^*} \leq \sqrt{\gamma} \leq \lambda_{n-1}, \\ \lambda_{n-1} + \frac{\gamma}{\lambda_{n-1}}, & \text{if } \lambda_{n-1} < \sqrt{\gamma}. \end{cases}$$

Moreover, $\gamma \mapsto \Lambda_-$ is continuous.

Proof. First note that, since G is connected, for all $m \in \{1, \dots, n-1\}$, $\Lambda_m > 0$, hence $\Lambda_- > 0$. Furthermore, if $\lambda_1 \leq \sqrt{\gamma} \leq \lambda_{n-1}$, then the sets in the definitions of λ_* and λ^* are nonempty and thus λ_* and λ^* are well-defined. Following from the discussion in Remark 5.5 we know that $x \mapsto x + \frac{\gamma}{x}$ is either non-increasing, non-decreasing, or it achieves its unique minimum on $(0, \infty)$ at $x = \sqrt{\gamma}$, depending on the value of γ. Hence the minimum value of Λ_m ($m \geq 1$) is achieved when either $m = 1$, $m = n-1$, or m is such that $\lambda_m = \lambda_*$ or $\lambda_m = \lambda^*$. By the argument in Remark 5.5 we know that the first two cases occur when $\lambda_1 \geq \sqrt{\gamma}$ or $\lambda_{n-1} \leq \sqrt{\gamma}$, respectively. The other two cases follow from

$$\lambda_* + \frac{\gamma}{\lambda^*} < \lambda^* + \frac{\gamma}{\lambda^*} \Leftrightarrow \gamma < \frac{\lambda_* - \lambda^*}{\frac{1}{\lambda^*} - \frac{1}{\lambda_*}} = \lambda_* \lambda^*.$$

Note that if $\lambda_1 = \sqrt{\gamma}$, then $\sqrt{\lambda_* \lambda^*} = \lambda_1$; if $\lambda_{n-1} = \sqrt{\gamma}$, then $\sqrt{\lambda_* \lambda^*} = \lambda_{n-1}$; if $\lambda_* \lambda^* = \gamma$, then $\lambda_* + \frac{\gamma}{\lambda_*} = \lambda^* + \frac{\gamma}{\lambda_*}$. Thus $\gamma \mapsto \Lambda_-$ is continuous. □

Lemma 5.8. *Let $G = (V, E, \omega) \in \mathcal{G}$ and let λ_m ($m \in \{0, \dots, n-1\}$) be the eigenvalues of Δ as in (M35). Then the spectral radius of L as defined in Definition 5.6 is*

$$\Lambda_+ = \begin{cases} \lambda_1 + \frac{\gamma}{\lambda_1}, & \text{if } \lambda_1 \lambda_{n-1} < \gamma, \\ \lambda_{n-1} + \frac{\gamma}{\lambda_{n-1}}, & \text{if } \lambda_1 \lambda_{n-1} \geq \gamma. \end{cases}$$

Moreover, $\gamma \mapsto \Lambda_+$ is continuous.

Proof. First we note that, by Lemma M5.8 all eigenvalues Λ_m of L are nonnegative. Since G is connected and $n \geq 2$, there is at least one positive eigenvalue, so $\Lambda_+ > 0$. By the computation in Remark 5.5 the function $x \mapsto x + \frac{\gamma}{x}$ is either non-increasing, non-decreasing, or strictly convex on the domain $(0, \lambda_{n-1})$, depending on the value of γ. Thus, by the expression for Λ_m in Lemma M5.8, we see that the maximum value of Λ_m is achieved when either $m = 1$ or $m = n-1$, depending on the value of γ. If $\lambda_1 = \lambda_{n-1}$, then $\Lambda_1 = \Lambda_{n-1}$ and the result follows. If $\lambda_1 \neq \lambda_{n-1}$, then $\frac{1}{\lambda_{n-1}} - \frac{1}{\lambda_1} < 0$, hence we compute

$$\lambda_1 + \frac{\gamma}{\lambda_1} > \lambda_{n-1} + \frac{\gamma}{\lambda_{n-1}} \Leftrightarrow \gamma > \frac{\lambda_1 - \lambda_{n-1}}{\frac{1}{\lambda_{n-1}} - \frac{1}{\lambda_1}} = \lambda_1 \lambda_{n-1}.$$

Replacing the inequality by an equality, shows continuity of $\gamma \mapsto \Lambda_+$. □

Lemma 5.9. *Let $G \in \mathcal{G}$, $\gamma \geq 0$, and $u_0 \in \mathcal{V}$. If $u \in \mathcal{V}_\infty$ is a solution of (M47), with corresponding $\varphi \in \mathcal{V}_\infty$, then, for all $t > 0$,*

$$\frac{d}{dt} \|u(t)\|_{\mathcal{V}}^2 = -2 \left(\|\nabla u(t)\|_{\mathcal{E}}^2 + \gamma \|\nabla \varphi\|_{\mathcal{E}}^2 \right) \leq 0.$$

In particular, for all $t \geq 0$, $\|u(t)\|_{\mathcal{V}} \leq \|u_0\|_{\mathcal{V}}$.

Moreover, if $\eta > 0$ and $t' > \Lambda_-^{-1} \log \left(\eta^{-1} d_-^{-\frac{r}{2}} \|u_0 - \mathcal{A}(u_0)\|_{\mathcal{V}} \right)$, where Λ_- is as in Lemma 5.7, then for all $t > t'$, $\|u(t) - \mathcal{A}(u(t))\|_{\mathcal{V},\infty} < \eta$.

Proof. This proof follows very closely the proof of [vGGOB14, Lemma 2.6(b) and (c)].

We compute

$$\frac{d}{dt}\|u(t)\|_{\mathcal{V}}^2 = 2\langle u(t), \frac{\partial}{\partial t}u(t)\rangle_{\mathcal{V}} = -2\langle u(t), L\left(u(t)\right)\rangle_{\mathcal{V}} = -2\left(\langle u(t), \Delta u(t)\rangle_{\mathcal{V}} + \gamma\langle u(t), \varphi(t)\rangle_{\mathcal{V}}\right).$$

Since $\mathcal{M}(\varphi) = 0$, we have $\langle \mathcal{A}(u(t)), \varphi\rangle_{\mathcal{V}} = 0$ and thus $\langle u(t), \Delta u(t)\rangle_{\mathcal{V}} = \langle \nabla u(t), \nabla u(t)\rangle_{\mathcal{V}}$ and

$$\langle u(t), \varphi(t)\rangle_{\mathcal{V}} = \langle u(t) - \mathcal{A}(u(t)), \varphi(t)\rangle_{\mathcal{V}} = \langle \Delta\varphi(t), \varphi(t)\rangle_{\mathcal{V}} = \langle \nabla\varphi(t), \nabla\varphi(t)\rangle_{\mathcal{V}},$$

from which the expression for $\frac{d}{dt}\|u(t)\|_{\mathcal{V}}^2$ follows.

To prove the final statement we expand $u(t) - \mathcal{A}(u(t)) = \sum_{m=1}^{n-1} e^{-t\Lambda_m}\langle u_0, \phi^m\rangle_{\mathcal{V}}\,\phi^m$. Let $t > 0$. Recall that the eigenfunctions ϕ^m are pairwise $\mathcal{V}$-orthogonal, hence

$$\begin{aligned}\left\|\sum_{m=1}^{n-1} e^{-t\Lambda_m}\langle u_0, \phi^m\rangle_{\mathcal{V}}\,\phi^m\right\|_{\mathcal{V}}^2 &= \sum_{m=1}^{n-1}\left\|e^{-t\Lambda_m}\langle u_0, \phi^m\rangle_{\mathcal{V}}\,\phi^m\right\|_{\mathcal{V}}^2 \\ &\le e^{-2t\Lambda_-}\sum_{m=1}^{n-1}\|\langle u_0, \phi^m\rangle_{\mathcal{V}}\,\phi^m\|_{\mathcal{V}}^2 = e^{-2t\Lambda_-}\left\|\sum_{m=1}^{n-1}\langle u_0, \phi^m\rangle_{\mathcal{V}}\,\phi^m\right\|_{\mathcal{V}}^2.\end{aligned}$$

Therefore $\|u(t)-\mathcal{A}(u(t))\|_{\mathcal{V}} \le e^{-t\Lambda_-}\left\|\sum_{m=1}^{n-1}\langle u_0, \phi^m\rangle_{\mathcal{V}}\,\phi^m\right\|_{\mathcal{V}} = e^{-t\Lambda_-}\|u_0 - \mathcal{A}(u_0)\|_{\mathcal{V}}$. By (M3) we conclude that $\|u(t) - \mathcal{A}(u(t))\|_{\mathcal{V},\infty} \le d_-^{-\frac{r}{2}}\|u(t) - \mathcal{A}(u(t))\|_{\mathcal{V}} \le d_-^{-\frac{r}{2}}e^{-t\Lambda_-}\|u_0 - \mathcal{A}(u_0)\|_{\mathcal{V}} < \eta$. □

5.3 Pinning and spreading

The following lemma and its proof use some of the results above and follow very closely [vGGOB14, Theorems 4.2, 4.3, 4.4]. The lemma gives sufficient bounds on the parameter τ for the M(OKMBO) dynamics to be 'uninteresting', i.e. for the evolution to be either pinned (i.e. each iteration gives back the initial set) or for the dynamics in (M47) to spread the mass so widely that M(OKMBO) arrives at a trivial (constant) stationary state in one iteration. In the lemma's proof, we need an operator norm, which, for a linear operator $O : \mathcal{V} \to \mathcal{V}$, we define as

$$\|O\|_o := \max_{\mathcal{V}\setminus\{0\}} \frac{\|Ou\|_{\mathcal{V}}}{\|u\|_{\mathcal{V}}}.$$

A property of this norm is that, for all $u \in \mathcal{V}$, $\|Ou\|_{\mathcal{V}} \le \|O\|_o\|u\|_{\mathcal{V}}$.

Since L is self-adjoint, it follows from the Rayleigh quotient formulation of $L's$ eigenvalues, that $\|L\|_o = \Lambda_+$, where Λ_+ is the spectral radius of L as in Lemma 5.8 [RS, Theorem. VI.6].

Lemma 5.10. *Let $G = (V, E, \omega) \in \mathcal{G}$. Let $\gamma \ge 0$ and let Λ_- and Λ_+ be as in Lemma 5.7 and Lemma 5.8, respectively. Let $S \subset V$. If $S \ne \emptyset$, define*

$$\tau_\rho(S) := \Lambda_+^{-1}\log\left(1 + \frac{1}{2}d_-^{\frac{r}{2}}\left(\mathrm{vol}\,(S)\right)^{-\frac{1}{2}}\right).$$

If in addition $S \ne V$ and $\frac{\mathrm{vol}(S)}{\mathrm{vol}(V)} \ne \frac{1}{2}$, also define

$$\tau_t(S) := \Lambda_-^{-1}\log\left(\frac{\left(\mathrm{vol}\,(S)\right)^{\frac{1}{2}}\left(\mathrm{vol}\,(S^c)\right)^{\frac{1}{2}}}{\left(\mathrm{vol}\,(V)\right)^{\frac{1}{2}}\left|\frac{\mathrm{vol}(S)}{\mathrm{vol}(V)} - \frac{1}{2}\right| d_-^{\frac{r}{2}}}\right).$$

Let $\gamma \ge 0$, $\tau > 0$, and S^1 be the first set in the corresponding M(OKMBO) evolution of the initial set $S^0 = S$.

1. *If $\tau < \tau_\rho(S)$, then $S^1 = S$. In particular, if $\tau < \Lambda_+^{-1}\log\frac{3}{2} \approx 0.4\Lambda_+^{-1}$, then $S^1 = S$.*

2. *If* $\emptyset \neq S \neq V$, $\frac{\mathrm{vol}(S)}{\mathrm{vol}(V)} \neq \frac{1}{2}$, *and* $\tau > \tau_t(S)$, *then* $S^1 = \begin{cases} \emptyset, & \text{if } \frac{\mathrm{vol}(S)}{\mathrm{vol}(V)} < \frac{1}{2}, \\ V, & \text{if } \frac{\mathrm{vol}(S)}{\mathrm{vol}(V)} > \frac{1}{2}. \end{cases}$

If $S = \emptyset$ *or* $S = V$, *then* $S^1 = S$.

Moreover, if $\emptyset \neq S \neq V$, $\frac{\mathrm{vol}(S)}{\mathrm{vol}(V)} \neq \frac{1}{2}$, *and* $\frac{\Lambda_-}{\Lambda_+} < \frac{\log\sqrt{2}}{\log\frac{3}{2}} \approx 0.85$, *then* $\tau_\rho(S) < \tau_t(S)$.

Proof. The proof follows very closely the proofs of [vGGOB14, Theorems 4.2, 4.3, 4.4], but we include it here for completeness.

To prove 1, first let $\tau < \tau_\rho(S)$. Let $\mathrm{Id} : \mathcal{V} \to \mathcal{V}$ be the identity operator, then we compute the operator norm $\|e^{-\tau L} - \mathrm{Id}\|_o \leq \sum_{j=1}^{\infty} \frac{1}{j!} (\tau \|L\|_o)^j = e^{\rho t} - 1 < \frac{1}{2} d_-^{\frac{r}{2}} (\mathrm{vol}\,(S))^{-\frac{1}{2}}$, where we used the triangle inequality and submultiplicative property of $\|\cdot\|_o$ [HJ90] for the first inequality. Hence, by (M3),

$$\begin{aligned} \|e^{-\tau L}\chi_S - \chi_S\|_{\mathcal{V},\infty} &\leq d_-^{-\frac{r}{2}} \|e^{-\tau L}\chi_S - \chi_S\|_{\mathcal{V}} \leq d_-^{-\frac{r}{2}} \|e^{-\tau L} - \mathrm{Id}\|_{\mathcal{V}} \|\chi_S\|_{\mathcal{V}} \\ &= d_-^{-\frac{r}{2}} \|e^{-\tau L} - \mathrm{Id}\|_{\mathcal{V}} \sqrt{\mathrm{vol}\,(S)} < \frac{1}{2}. \end{aligned}$$

It follows from the thresholding step in M(OKMBO) that $S^1 = S$.

To prove 2 (for any $r \in [0,1]$), we use Lemma 5.9 with $\eta := \left|\frac{\mathrm{vol}(S)}{\mathrm{vol}(V)} - \frac{1}{2}\right|$ to find

$$\left| \|u(\tau)\|_{\mathcal{V},\infty} - \mathcal{A}(\chi_S) \right| \leq \|u(\tau) - \mathcal{A}(\chi_S)\|_{\mathcal{V},\infty} < \left| \frac{\mathrm{vol}\,(S)}{\mathrm{vol}\,(V)} - \frac{1}{2} \right|.$$

If $\frac{\mathrm{vol}(S)}{\mathrm{vol}(V)} < \frac{1}{2}$ this implies

$$\|u(\tau)\|_{\mathcal{V},\infty} \leq \|u(\tau) - \mathcal{A}(\chi_S)\|_{\mathcal{V},\infty} + \|\mathcal{A}(\chi_S)\|_{\mathcal{V},\infty} < \left| \frac{\mathrm{vol}\,(S)}{\mathrm{vol}\,(V)} - \frac{1}{2} \right| + \frac{\mathrm{vol}\,(S)}{\mathrm{vol}\,(V)} = \frac{1}{2}.$$

Alternatively, if $\frac{\mathrm{vol}(S)}{\mathrm{vol}(V)} > \frac{1}{2}$, then

$$\frac{\mathrm{vol}\,(S)}{\mathrm{vol}\,(V)} = \|\mathcal{A}(\chi_S)\|_{\mathcal{V},\infty} \leq \|u(\tau) - \mathcal{A}(\chi_S)\|_{\mathcal{V},\infty} + \|u(\tau)\|_{\mathcal{V},\infty} < \frac{\mathrm{vol}\,(S)}{\mathrm{vol}\,(V)} - \frac{1}{2} + \|u(\tau)\|_{\mathcal{V},\infty},$$

and thus $\|u(\tau)\|_{\mathcal{V},\infty} > \frac{1}{2}$. The result then follows from the thresholding step in M(OKMBO).

Since $L\chi_\emptyset = \chi_\emptyset$ and $L\chi_V = \chi_V$, the subsets $S = \emptyset$ and $S = V$ are stationary states of the ODE step in m(OKMBO) and thus $S^1 = S$.

To prove the final statement, we first note that, since $\emptyset \neq S \neq V$, we have $d_-^r \leq \mathrm{vol}\,(S) \leq \mathrm{vol}\,(V) - d_-^r$. Since $(\mathrm{vol}\,(S))(\mathrm{vol}\,(S^c)) = \mathrm{vol}\,(S)\,(\mathrm{vol}\,(V) - \mathrm{vol}\,(S))$ is concave as a function of $\mathrm{vol}\,(S)$, we find

$$\begin{aligned} (\mathrm{vol}\,(S))(\mathrm{vol}\,(S^c)) &\geq \min\{d_-^r \left(\mathrm{vol}\,(V) - d_-^r\right), \left(\mathrm{vol}\,(V) - d_-^r\right) \left(\mathrm{vol}\,(V) - \left(\mathrm{vol}\,(V) - d_-^r\right)\right)\} \\ &= d_-^r \left(\mathrm{vol}\,(V) - d_-^r\right). \end{aligned}$$

We also note that $\left|\frac{\mathrm{vol}(S)}{\mathrm{vol}(V)} - \frac{1}{2}\right| \leq \frac{1}{2}$. Hence $\tau_\rho(S) \leq \Lambda_+^{-1} \log\left(\frac{3}{2}\right)$ and $\tau_t(S) \geq \Lambda_- \log\left(2\sqrt{1 - \frac{d_- r}{\mathrm{vol}(S)}}\right) \leq \Lambda^{-1} \log\sqrt{2}$, where the last inequality follows from $\mathrm{vol}\,(V) \geq n d_-^r \geq 2 d_-^r$. □

Remark 5.11. The exclusion of the case $\mathrm{vol}\left(S^0\right) = \frac{1}{2}\mathrm{vol}\,(V)$ for the establishment of τ_t in Lemma 5.10 is a necessary one, as in this case symmetry could lead to pinning in M(OKMBO), such that $S^1 = S^0$ (and thus $\emptyset \neq S^1 \neq V$). For example, consider an unweighted, completely connected graph and an initial set S^0 such that $\mathrm{vol}\left(S^0\right) = \frac{1}{2}\mathrm{vol}\,(V)$. By symmetry, no nontrivial dynamics can occur, regardless of the value of τ; hence $e^{-\tau L}\chi_{S^0} = \chi_{S^0}$ and thus $S^1 = S^0$.

6 Star graph and other examples

Throughout the paper we will use the example of a star graph to illustrate various ideas, because it is amenable to analytical calculations. We therefore give its definition here and introduce the notation we will be using for it.

Definition 6.1. *A (weighted) undirected simple graph $G = (V, E, \omega)$ is complete if, for all $i, j \in V$, $i \neq j$ implies $\omega_{ij} > 0$.*

A (weighted) undirected simple graph $G = (V, E, \omega)$ is bipartite if there are disjoint subsets V_1 and V_2 of V such that $V = V_1 \cup V_2$ and for all $i, j \in V_1$ and for all $k, l \in V_2$, $\omega_{ij} = \omega_{kl} = 0$. In this case we write $V = V_1 | V_2$.

A bipartite graph with node set $V = V_1 | V_2$ is called a complete bipartite graph if, for all $i \in V_1$ and for all $j \in V_2$, $\omega_{ij} > 0$.

A (weighted) undirected simple graph $G = (V, E, \omega)$ is a (weighted) star graph if it is a complete bipartite graph with $V = V_1 | V_2$ and $|V_1| = 1$ or $|V_2| = 1$. The single node in V_1 or V_2, respectively, is the centre node or internal node. The other nodes, in V_2 or V_1, respectively, are leaf nodes (or leaves).

For a (weighted) star graph we will use the notational convention that $1 \in V$ is the centre node and $\{2, \dots, n\}$ is the set of leaves, i.e. for all $i \in V$, $\omega_{ii} = 0$, for all $j \in V \setminus \{1\}$, $\omega_{1j} = 1$, and if $i, j \in V \setminus \{1\}$, then $\omega_{ij} = 0$.

See Figure 1 for an example of a star graph.

The following lemma describes $\mathfrak{M}$ for star graphs and shows that the mass condition in $\mathcal{V}_M^b$ can be quite restrictive, especially if $r \neq 0$.

Lemma 6.2. *Let $G = (V, E, \omega) \in \mathcal{G}$ be an unweighted star graph as in Definition 6.1 with $n \geq 3$ nodes and let $q = 1$. Let $\mathfrak{M}$ be the set of admissable masses as in (M11), then*

$$\mathfrak{M} = \{0, 1, \dots, n-1, (n-1)^r, (n-1)^r + 1, \dots, (n-1)^r + n - 1\}.$$

- *If $(n-1)^r \notin \mathbb{N}$ and $M \in \mathfrak{M} \cap \mathbb{N}$, then for all $\chi_S \in \mathcal{V}_M^b$ (with $S \subset V$), $1 \notin S$ and $|S| = M$.*
- *If $(n-1)^r \notin \mathbb{N}$ and $M \in \mathfrak{M} \cap (\mathbb{R} \setminus \mathbb{N})$, then for all $\chi_S \in \mathcal{V}_M^b$, $1 \in S$ and $|S \setminus \{1\}| = M - 1$.*
- *If $M \in \mathfrak{M} \cap [0, (n-1)^r)$, then for all $\chi_S \in \mathcal{V}_M^b$, $1 \notin S$.*
- *If $M \in \mathfrak{M} \cap (n-1, \mathrm{vol}\,(V)]$, then for all $\chi_S \in \mathcal{V}_M^b$, $1 \in S$.*
- *If $M \in \mathfrak{M}$ and $\chi_S, \chi_{\tilde{S}} \in \mathcal{V}_M^b$ are such that $(\chi_S)_1 = (\tilde{\chi}_S)_1$, then $|S| = |\tilde{S}|$.*

Proof. Let $u \in \mathcal{V}_M^b$, then $\mathcal{M}(u) = (n-1)^r u_1 + \sum_{i=2}^n u_i$, from which the expression for $\mathfrak{M}$ immediately follows.

If $(n-1)^r \notin \mathbb{N}$ and $M \in \mathfrak{M} \cap \mathbb{N}$, then $M \in \{0, 1, \dots, n-1\}$, hence $1 \notin S$ and $|S| = M$. If on the other hand $(n-1)^r \notin \mathbb{N}$ and $M \in \mathfrak{M} \cap (\mathbb{R} \setminus \mathbb{N})$, then $M \in \{(n-1)^r, (n-1)^r + 1, \dots, (n-1)^r + n - 1\}$ and thus $1 \in S$ and $|S \setminus \{1\}| = M - 1$.

If $M \in \mathfrak{M}$ satisfies $M < (n-1)^r$, then $\mathcal{M}(\chi_S) = M$ implies $1 \notin S$. If on the other hand $M > n - 1$ and $1 \notin S$, then $\mathcal{M}(\chi_S) \leq n - 1 < M$, hence $\chi_S \notin \mathcal{V}_M^b$.

If $\mathcal{M}(\chi_S) = \mathcal{M}(\chi_{\tilde{S}})$ and $(\chi_S)_1 = (\chi_{\tilde{S}})_1$, then

$$|S| - |\tilde{S}| = (\chi_S)_1 - \sum_{i=2}^n (\chi_S)_i - (\chi_{\tilde{S}})_1 - \sum_{i=2}^n (\chi_{\tilde{S}})_i = \sum_{i=2}^n (\chi_S)_i - \sum_{i=2}^n (\chi_{\tilde{S}})_i = \mathcal{M}(\chi_S) - \mathcal{M}(\chi_{\tilde{S}}) = 0.$$

□

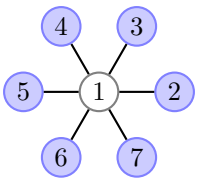

Figure 1: An example of a star graph with six leaf nodes

Remark 6.3. If $r = 0$, the assumptions in the first four bullet points of Lemma 6.2 cannot be satisfied and the condition $M \in \mathfrak{M}$ is less restrictive than in the case $r \in (0, 1]$.

The following lemmas give examples of explicitly constructed equilibrium measures on a bipartite graph and a star graph.

Lemma 6.4. *Let $G = (V, E, \omega) \in \mathcal{G}$ be a bipartite graph with $V = V_1 | V_2$. Let $S \subset V_1$ and let ν^S be the equilibrium measure for S, as in Definition M3.3. Then $\nu_i^S = d_i^{r-1}(\chi_S)_i$.*

Proof. Since $n \geq 2$ and G is connected, S is a proper subset of V. Per definition we have, for all $i \in S^c$, $\nu_i^S = 0$. In particular this holds for all $i \in V_2 \subset S^c$, hence, for all $j \in S \subset V_1$ we compute

$$1 = (\Delta \nu^S)_j = d_j^{-r} \sum_{k \in V_2} \omega_{jk} \left(\nu_j^S - \nu_k^S \right) = d_j^{1-r} \nu_j^S.$$

□

Lemma 6.5. *Let $G = (V, E, \omega) \in \mathcal{G}$ be an unweighted star graph with $n \geq 3$ nodes as in Definition 6.1. If $j = 1 \in V$, then the equilibrium measure for $V \setminus \{1\}$, as defined in Definition M3.3, is given by, for all $i \in V$,*

$$\nu_i^{V \setminus \{1\}} = \begin{cases} 0, & \text{if } i = 1, \\ 1, & \text{if } i \neq 1. \end{cases}$$

If $j \in V \setminus \{1\}$, the equilibrium measure for $V \setminus \{j\}$ is given by

$$\nu_i^{V \setminus \{j\}} = \begin{cases} 0, & \text{if } i = j, \\ \operatorname{vol}(V) - 1 = (n-1)^r + n - 2, & \text{if } i = 1, \\ \operatorname{vol}(V) = (n-1)^r + n - 1, & \text{if } i \neq j \text{ and } i \neq 1. \end{cases}$$

Proof. In the case where $j = 1$, the result follows immediately from Lemma 6.4 with $d_i^{r-1} = 1$ for $i \neq 1$ and $r \in [0, 1]$.

Next let $j \neq 1$, then

$$\begin{aligned} \left(\Delta \nu^{V \setminus \{j\}} \right)_1 &= (n-1)^{-r} \left((n-1) \nu_1^{V \setminus \{j\}} - \nu_j^{V \setminus \{j\}} - \sum_{k \in V \setminus \{1, j\}} \nu_k^{V \setminus \{j\}} \right) \\ &= (n-1)^{-r} \left((n-1)^{r+1} + (n-1)(n-2) - (n-2)(n-1)^r - (n-2)(n-1) \right) \\ &= (n-1) - (n-2) = 1, \end{aligned}$$

where we used that $d_1 = n - 1$. Moreover, if $i \neq 1 \neq j$, then

$$\left(\Delta \nu^{V \setminus \{j\}} \right)_i = d_i^{-r} \left((n-1)^r + n - 1 - (n-1)^r - n + 2 \right) = 1,$$

since $d_i = 1$. Thus $\nu^{V \setminus \{j\}}$ solves (M12) for $S = V \setminus \{j\}$.

Finally we note that $\operatorname{vol}(V) = d_1^r + \sum_{i \in V \setminus \{1\}} d_i^r = (n-1)^r + n - 1$. □

Remark 6.6. We can use the equilibrium measure we computed for the bipartite graph and star graph in Lemma 6.4 and Lemma M6.5, respectively, to illustrate the result from Lemma M3.6.

For the bipartite graph from Lemma 6.4 and $S \subset V_1$, we compute, for all $i \in S$, $(\kappa_S)_i = d_i^{-r+1} = \left(\nu_i^S \right)^{-1}$. This shows that the result from Lemma M3.6 is sharp, in the sense that there is no greater lower bound for ν^S on S which holds for every $G \in \mathcal{G}$.

For the star graph from Lemma 6.5 we compute, for $i \in V \setminus \{1\}$, $\left(\kappa_{V \setminus \{1\}} \right)_i = d_i^{-r+1} = 1$. It is not surprising that this is another occasion in which equality is achieved in the bound from Lemma M3.6, as this situation is a special case of the bipartite graph result. The case when $j \neq 1$, however, shows that equality is not always achieved. In this case, if $i \in V \setminus \{j\}$, then $\left(\kappa_{V \setminus \{j\}} \right)_i = d_i^{-r} \omega_{ij}$. Since $\omega_{1j} = 1$ and, if $i \neq 1$, $\omega_{ij} = 0$, we have $\kappa^+_{V \setminus \{j\}} = (n-1)^{-r}$, so $\nu^{V \setminus \{j\}} > \left(\kappa^+_{V \setminus \{j\}} \right)^{-1}$ on $V \setminus \{j\}$.

Lemma 6.7 below describes a symmetry in F_0 when the underlying graph is a star graph; in a sense it is an extension of the last statement in Lemma 6.2. It will come in handy later.

Lemma 6.7. *Let $G = (V, E, \omega)$ be an unweighted star graph as in Definition 6.1 with $n \geq 3$ nodes and let $q = 1$. Let $\mathfrak{M}$ be the set of admissable masses as in (M11). If $S, \tilde{S} \subset V$ are such that $|S| = |\tilde{S}|$ and $(\chi_S)_1 = (\chi_{\tilde{S}})_1$, then $F_0(\chi_S) = F_0(\chi_{\tilde{S}})$, where F_0 is the limit Ohta-Kawasaki functional from (M32).*

Proof. Let $S, \tilde{S} \subset V$ be such that $|S| = |\tilde{S}|$ and $(\chi_S)_1 = (\chi_{\tilde{S}})_1$. Because the unweighted star graph G is symmetric under permutations of its leaves (i.e. the nodes $\{2, \ldots, n\}$), for any $u \in \mathcal{V}^b$ the value of $F_0(u)$ depends only on the value of u_1 and the number of leaves i for which $u_i = 0$. Hence $F_0(\chi_S) = F_0(\chi_{\tilde{S}})$. □

Next we give Laplacian eigenvalues and eigenfunctions as in (M35) and (M36) for star graphs.

Lemma 6.8. *Let $G = (V, E, \omega)$ be an unweighted star graph as in Definition 6.1 with $n \geq 3$ nodes. The eigenvalues are*[3]

$$\lambda_0 = 0, \qquad \lambda_m = 1 \quad (m \in \{1, \ldots, n-2\}), \qquad \lambda_{n-1} = (n-1)^{1-r} + 1.$$

A corresponding $\mathcal{V}$-orthonormal system of eigenfunctions is given by, for $m \in \{1, \ldots, n-2\}$ and $i \in \{1, \ldots, n\}$,

$$\begin{aligned}
\phi^0 &= \left[(n-1)^{1-r} + n - 1\right]^{-1/2} \chi_V, \\
\phi_i^m &= \left[(n-m-1)^2 + n - m - 1\right]^{-1/2} \begin{cases} 0, & \text{if } 1 \leq i \leq m, \\ n-m-1, & \text{if } i = m+1, \\ -1, & \text{if } m+2 \leq i \leq n, \end{cases} \\
\phi_i^{n-1} &= \left[(n-1)^{2-r} + n - 1\right]^{-1/2} \begin{cases} (n-1)^{1-r}, & \text{if } i = 1, \\ -1, & \text{if } 2 \leq i \leq n, \end{cases}
\end{aligned}$$

where the subscript i indicates the component of the vector.

Proof. The eigenvalues and eigenvectors were found following a computation similar to that in [vGGOB14, Section 6.2], but for this proof a direct computation suffices to show that $\langle \phi^m, \phi^l \rangle_{\mathcal{V}} = \delta_{ml}$ and $\Delta \phi^m = \lambda_m \phi^m$. □

Lemma 6.8 and Corollary M4.12 allow us to explicitly give the Ohta-Kawasaki functional for our star graph example from Definition 6.1.

Lemma 6.9. *Let $G = (V, E, \omega)$ be an unweighted star graph as in Definition 6.1 with $n \geq 3$ and let $q = 1$. Let $S \subset V$. For $l \in \mathbb{N}$ define $N_l(S) := |\{i \in S : i \geq l\}|$. Then*

$$\begin{aligned}
F_0(\chi_S) = &\sum_{l=2}^{n-1} \frac{1+\gamma}{(n-l)(n-l+1)} \left[(n-l)(\chi_S)_l - N_{l+1}(S)\right]^2 \\
&+ \frac{1}{n-1} \left(1 + \frac{\gamma}{((n-1)^{1-r}+1)^2}\right) \left[(n-1)(\chi_S)_1 - N_2(S)\right]^2.
\end{aligned}$$

Proof. This follows by combining the eigenfunctions and eigenvalues we found in Lemma 6.8 with (M44).

[3] If all the edges are given the same weight $\omega > 0$ instead of 1, it is quickly checked that all eigenvalues are multiplied by ω^{1-r}, because the Laplacian is multiplied by the same factor. Since in that case the factor d_i^r in the $\mathcal{V}$-inner product changes by a factor ω^r, the eigenfunctions all acquire a multiplicative factor $\omega^{-r/2}$.

Define, for $k \in \mathbb{N}$, $I(k) := \{i \in \mathbb{N} : k \leq i \leq n\}$. Then we compute, for $m \in \{1, \dots, n-2\}$,

$$\begin{aligned}
\langle \chi_S, \phi^m \rangle_{\mathcal{V}}^2 &= \frac{1}{(n-m-1)(n-m)} \sum_{i,j \in S} \Big[(n-m-1)^2 \delta_{i,m+1}\delta_{j,m+1} + \left(\chi_{I(m+2)}\right)_i \left(\chi_{I(m+2)}\right)_j \\
&\qquad - (n-m-1)\left(\delta_{i,m+1}\left(\chi_{I(m+2)}\right)_j + \delta_{j,m+1}\left(\chi_{I(m+2)}\right)_i\right)\Big] \\
&= \frac{n-m-1}{n-m}\left(\chi_S\right)_{m+1} + \frac{1}{(n-m-1)(n-m)}\left(\sum_{i=m+2}^{n}\left(\chi_S\right)_i\right)^2 \\
&\qquad - \frac{2}{n-m}\left(\chi_S\right)_{m+1}\sum_{i=m+2}^{n}\left(\chi_S\right)_i, \\
\langle \chi_S, \phi^{n-1} \rangle_{\mathcal{V}}^2 &= \frac{1}{(n-1)\left((n-1)^{1-r}+1\right)} \sum_{i,j \in S} d_i^r d_j^r \Big[(n-1)^{2-2r}\delta_{i1}\delta_{j1} + \left(\chi_{I(2)}\right)_i \left(\chi_{I(2)}\right)_j \\
&\qquad - (n-1)^{1-r}\left(\delta_{i1}\left(\chi_{I(2)}\right)_j + \delta_{j1}\left(\chi_{I(2)}\right)_i\right)\Big] \\
&= \frac{n-1}{(n-1)^{1-r}+1}\left(\chi_S\right)_1 + \frac{1}{(n-1)\left((n-1)^{1-r}+1\right)}\left(\sum_{i=2}^{n}\left(\chi_S\right)_i\right)^2 \\
&\qquad - \frac{2}{(n-1)^{1-r}+1}\left(\chi_S\right)_1\sum_{i=2}^{n}\left(\chi_S\right)_i.
\end{aligned}$$

Substituting these into (M44) and noting that $N_l(S) = \sum_{i=l}^{n}\left(\chi_S\right)_i$ gives the desired result. □

We are now in a position to solve the minimization problem from (M34) for star graphs.

Corollary 6.10. *Let $G = (V, E, \omega)$ be an unweighted star graph as in Definition 6.1 with $n \geq 3$ nodes, with spectrum as in Lemma 6.8, and let $q = 1$. Let $\mathfrak{M}$ be the set of admissable masses as in (M11). Let $M \in \mathfrak{M}$ be such that there are $u, \tilde{u} \in \mathcal{V}_M^b$ with $u_1 = 0$ and $\tilde{u}_1 = 1$. Consider the minimization problem from (M34). We have*

- *if $M = \frac{1}{2}\mathrm{vol}\,(V)$ or $\gamma = \lambda_{n-1}$, then all $u \in \mathcal{V}_M^b$ are minimizers of (M34);*
- *if $(\mathrm{vol}\,(V) - 2M)(\gamma - \lambda_{n-1}) < 0$, then $u \in \mathcal{V}_M^b$ is a minimizer of (M34) if and only if $u_1 = 0$;*
- *if $(\mathrm{vol}\,(V) - 2M)(\gamma - \lambda_{n-1}) > 0$, then $u \in \mathcal{V}_M^b$ is a minimizer of (M34) if and only if $u_1 = 1$.,*

Proof. For $w \in \mathcal{V}$, define $\ell(w) := |\{i \in \{2, \dots, n\} : w_i = 1\}|$, i.e. $\ell(w)$ is the number of leaf nodes on which w takes the value 1. By Lemma 6.7 we know that $F_0(w) = F_0(u)$ if $w_1 = 0$ and $F_0(w) = F_0(\tilde{u})$ if $w_1 = 1$. Thus, for each $w \in \mathcal{V}$ there is a $\hat{w} \in \mathcal{V}$ such that $F_0(w) = F_0(\hat{w})$, $\ell(w) = \ell(\hat{w})$, for all $i \in \{2, \dots, \ell(w)+1\}$ $\hat{w}_i = 1$, and (if $\ell(w) + 2 \leq n$) for all $i \in \{\ell(w)+2, \dots, n\}$ $\hat{w}_i = 0$. Hence, we assume without loss of generality that w satisfies the properties prescribed for $\hat{w}$ above. In particular, in the notation of Lemma 6.9, if $S = \{i \in V : w_i = 1\}$, then for $2 \leq l \leq n$, $N_l = \max(0, \ell(w) - (l-2))$. Substituting this in the expression for F_0 in Lemma 6.9 we find

$$\begin{aligned}
F_0(w) &= \sum_{l=2}^{\ell(w)+1} \frac{1+\gamma}{(n-l)(n-l+1)}\left((n-l) - (\ell(w) - (l-1))\right)^2 \\
&\qquad + \frac{1}{n-1}\left(1 + \frac{\gamma}{\left((n-1)^{1-r}+1\right)^2}\right)\left((n-1)w_1 - \ell(w)\right)^2 \\
&= \frac{1}{n-1}\left[(1+\gamma)\ell(w)(n-1-L) + \left(1 + \frac{\gamma}{\left((n-1)^{1-r}+1\right)^2}\right)\left((n-1)w_1 - \ell(w)\right)^2\right],
\end{aligned}$$

where for the second equality we used that

$$\sum_{l=2}^{\ell(w)+1} \frac{1+\gamma}{(n-l)(n-l+1)} = \frac{\ell(w)}{(n-1)(n-\ell(w)-1)}, \tag{4}$$

which in turn follows from Corollary 10.2 (whose proof is deferred to Section 10.4). Note that

$$M = (n-1)^r w_1 + \ell(w), \tag{5}$$

hence

$$F_0(w) = \frac{1}{n-1}\left[(1+\gamma)\left(n-1+(n-1)^r M w_1 - M\right)\left(M-(n-1)^r w_1\right) + \left(1+\frac{\gamma}{\left((n-1)^{1-r}+1\right)^2}\right)\left((n-1)w_1+(n-1)^r w_1 - M\right)^2\right].$$

If $w_1 = 0$ we compute

$$(n-1)F_0(u) = (n-1)F_0(w) = M^2\left(-(1+\gamma)+1+\frac{\gamma}{\left((n-1)^{1-r}+1\right)^2}\right) + (1+\gamma)(n-1)M.$$

If $w_1 = 1$ on the other hand, then

$$\begin{aligned}(n-1)F_0(\tilde{u}) &= (n-1)F_0(w) = \\ &M^2\left(-(1+\gamma)+1+\frac{\gamma}{\left((n-1)^{1-r}+1\right)^2}\right) \\ &+ M\left[-n+1+\gamma\left((n-1)^r\left(1+(n-1)^{1-r}\right)\left(1-\frac{2}{\left((n-1)^{1-r}+1\right)^2}\right)+(n-1)^r\right)\right] \\ &+ (1-\gamma)(n-1)^{1+r} + (n-1)^2.\end{aligned}$$

A short computation then shows that

$$F_0(u) - F_0(\tilde{u}) = \left(2M - \left((n-1)^r + n - 1\right)\right)\left(1 - \frac{\gamma}{(n-1)^{1-r}+1}\right).$$

Since $\mathrm{vol}\,(V) = (n-1)^r + n - 1$ and $\lambda_{n-1} = (n-1)^{1-r} + 1 > 0$ the results follow. □

Remark 6.11. We can easily understand the critical role that the value $M = \frac{1}{2}\mathrm{vol}\,(V)$ plays in Corollary 6.10. For any $S \subset V$ we have $\mathcal{M}(\chi_S) = \mathrm{vol}\,(V) - \mathcal{M}(\chi_{V\setminus S})$ and $F_0(\chi_S) = F_0(\chi_{V\setminus S})$, thus χ_S is a minimizer of (M34) for a given M, if and only if $\chi_{V\setminus S}$ is a minimizer for $\tilde{M} = \mathrm{vol}\,(V) - M$. We have $\tilde{M} = M$ if and only if $M = \frac{1}{2}\mathrm{vol}\,(V)$.

Furthermore, in Corollary 6.10 we found that $\gamma = \lambda_{n-1}$ is a critical value for star graphs at which the minimizer of F_0 changes its value at the internal node 1. This can heuristically be understood as the value of γ for which, for $m \in \{1,\dots,n-2\}$, $\lambda_m + \frac{\gamma}{\lambda_m} = \lambda_{n-1} + \frac{\gamma}{\lambda_{n-1}}$, and so the influence of ϕ^{n-1} —which is the eigenfunction that distinguishes node 1 from the other nodes— in (M44) becomes noticeable. It is not clear to what degree this heuristic can be applied to other graphs as well.

Remark 6.12. Note that in the star graph setting of Corollary 6.10 we assume that $M \in \mathfrak{M}$ is such that $\mathcal{V}^b_M$ contains both functions which take the value 0 on node 1 and functions which take the value 1 on node 1. If M were such that all functions in $\mathcal{V}^b_M$ took the same value on node 1, then minimizers of (M34) would be necessarily restricted to that class of functions and the 'if and only if' statements in the corollary would have to be weakened.

Notice, however, that this assumption can be quite restrictive. For example, when $r = 1$ we have that, if $M > n-1$, then all $u \in \mathcal{V}^b_M$ satisfy $u_1 = 1$, and if $M < n-1$, then all $u \in \mathcal{V}^b_M$ satisfy $u_1 = 0$. Hence, if $r = 1$, then the assumption from the corollary is satisfied if and only if $M = n-1 = \frac{1}{2}\mathrm{vol}\,(V)$, in which case the corollary tells us that all $u \in \mathcal{V}^b_M$ are minimizers of (M34).

In order to obtain a larger set of admissable masses with interesting behaviour, one could consider minimising $F_0(\chi_S)$ over all $\chi_S \in \mathcal{V}^b$ for which $|S| = M$, for a given $M \in (0,n) \cap \mathbb{N}$. Note that this problem is equivalent to (M34) if $r = 0$, but even if $r \neq 0$, any choice of $M \in (0,n) \cap \mathbb{N}$ will allow for admissible $u \in \mathcal{V}^b$ with $u_1 = 0$ and admissible $u \in \mathcal{V}^b$ with $u_1 = 1$. Of course it is a somewhat unnatural

mixture of conditions to set $r = 0$ in the mass condition, but not in the functional F_0. If we repeat the computation from the proof of Corollary 6.10 in this case, i.e. with $M = w_1 + L$ instead of (5), and define

$$g(\gamma) := (n - 2M)\left[\gamma\left(1 - \frac{n}{\lambda_{n-1}^2}\right) - (n-1)\right],$$

we find that if $g(\gamma) = 0$ all admissible u are minimizers; if $g(\gamma) < 0$ any admissible u is a minimizer if and only if $u_1 = 1$; and if $g(\gamma) > 0$ any admissible u is a minimizer if and only if $u_1 = 0$.

In Lemma 6.10 we saw that for unweighted star graphs the value of u_1 determines if $u \in \mathcal{V}$ is a minimizer of F_0 (with $q = 1$) or not (unless $M = \frac{1}{2}\mathrm{vol}\,(V)$ or $\gamma = \lambda_{n-1}$). It is therefore interesting to investigate the pinning behaviour of M(OKMBO) at the centre node of star graphs in more detail. In particular we are interested in the case where $1 \in S$ and $\left(e^{-\tau L}\chi_S\right)_1 \geq \frac{1}{2}$ and the case where $1 \notin S$ and $\left(e^{-\tau L}\chi_S\right)_1 < \frac{1}{2}$, as those are the cases in which the status of node 1 does not change after one iteration of M(OKMBO) (i.e. if $S^0 = S$, then either $1 \in S^0 \cap S^1$ or $1 \notin S^0 \cap S^1$). The following lemma gives explicit conditions on τ for these cases to occur.

Lemma 6.13. *Let $G = (V, E, \omega) \in \mathcal{G}$ be an unweighted star graph as in Definition 6.1 with $n \geq 3$ nodes. Let $\gamma \geq 0$, let $\Lambda_{n-1} = \lambda_{n-1} + \frac{\gamma}{\lambda_{n-1}}$ be the eigenvalue of L as in Lemma 6.8 and (M56), and let $S \subset V$. If $1 \in S$, then $\left(e^{-\tau L}\chi_S\right)_1 \geq \frac{1}{2}$ if and only if $\tau \geq 0$ is such that*

$$e^{-\Lambda_{n-1}\tau} \geq \frac{1}{2}\frac{\mathrm{vol}\,(V) - 2\mathcal{M}\,(\chi_S)}{\mathrm{vol}\,(V) - \mathcal{M}\,(\chi_S)}.$$

Alternatively, if $1 \notin S$ then $\left(e^{-\tau L}\chi_S\right)_1 < \frac{1}{2}$ if and only if $\tau \geq 0$ is such that

$$e^{-\Lambda_{n-1}\tau} > 1 - \frac{1}{2}\frac{\mathrm{vol}\,(V)}{\mathcal{M}\,(\chi_S)}.$$

It is worth remembering that in the setting of Lemma 6.13 we have $\mathrm{vol}\,(V) = (n-1)^r + n - 1$ and $\mathcal{M}\,(\chi_S) = (n-1)^r\,(\chi_S)_1 + |S \setminus \{1\}|$.

Proof of Lemma 6.13. The proof is a direct computation using an expansion as in (M38) along the lines of what was done in [vGGOB14, vG]. Using the spectrum in Lemma 6.8, we compute

$$\chi_S = \sum_{m=0}^{n-1}\langle\chi_S, \phi^m\rangle_{\mathcal{V}}\,\phi^m = \mathcal{A}\,(\chi_S) + \sum_{m=1}^{n-2}\langle\chi_S, \phi^m\rangle_{\mathcal{V}}\,\phi^m + \frac{(n-1)^{1-r}d_1^r\,(\chi_S)_1 - \sum_{i=2}^n d_i^r\,(\chi_S)_i}{(n-1)^{2-r} + n - 1}\phi^{n-1}.$$

Since $\Lambda_0 = 0$, for $m \in \{1, \ldots, n-2\}$, $\phi_1^m = 0$, $\phi_1^{n-1} = (n-1)^{1-r}$, $d_1^r = (n-1)^r$, for $i \in \{2, \ldots, n\}$, $d_i^r = 1$, and $\mathrm{vol}\,(V) = (n-1)^r + n - 1$, we compute

$$\begin{aligned}
\left(e^{-\tau L}\chi_S\right)_1 &= \sum_{m=0}^{n-1} e^{-\tau\Lambda_m}\langle\chi_S, \phi^m\rangle_{\mathcal{V}}\,\phi^m \\
&= \frac{\mathcal{M}\,(\chi_S)}{\mathrm{vol}\,(V)} + e^{-\tau\Lambda_{n-1}}\frac{(n-1)^{1-r}}{(n-1)^{2-r} + n - 1}\left((n-1)\,(\chi_S)_1 - \sum_{i=2}^n (\chi_S)_i\right) \\
&= \frac{1}{\mathrm{vol}\,(V)}\left[\mathcal{M}\,(\chi_S) + e^{-\tau\Lambda_{n-1}}\left(\mathrm{vol}\,(V)\,(\chi_S)_1 - \mathcal{M}\,(\chi_S)\right)\right].
\end{aligned}$$

The results in the lemma now follow by considering the cases $1 \in S$ and $1 \notin S$, hence $(\chi_S)_1 = 1$ and $(\chi_S)_1 = 0$, respectively. □

Remark 6.14. Interpreting the results from Lemma 6.13, we see that, for unweighted star graphs, if $1 \in S$, pinning at node 1 occurs for any value of $\tau \geq 0$ if $\mathcal{M}\,(\chi_S) \geq \frac{1}{2}\mathrm{vol}\,(V)$. If instead $1 \notin S$, then pinning at node 1 occurs, independent of the value of τ, if $\mathcal{M}\,(\chi_S) \leq \frac{1}{2}\mathrm{vol}\,(V)$. In particular, pinning at node 1 always occurs if $r = 1$, independent of the choice of τ or S.

7 Graphs in $\mathcal{C}$ and $\mathcal{C}^0$

The following lemma shows that the class of functions $\mathcal{C}$ is not empty (and thus, by Lemma M6.3 in the main paper, so are $\mathcal{C}^0$ and, for all $\gamma \geq 0$, $\mathcal{C}_\gamma$).

Lemma 7.1. *Let $G = (V, E, \omega) \in \mathcal{G}$ be an unweighted star graph as in Definition 6.1 with $n \geq 3$ nodes. Then $G \in \mathcal{C}$.*

Proof. Using Lemma 6.5, we compute

$$\begin{aligned}
\mathcal{M}\left(\nu^{V\setminus\{1\}}\right) &= \sum_{k\in V\setminus\{1\}} d_k^r = \operatorname{vol}(V) - d_1^r, \\
\mathcal{M}\left(\nu^{V\setminus\{j\}}\right) &= (\operatorname{vol}(V) - 1)d_1^r + \operatorname{vol}(V) \sum_{k\in V\setminus\{1,j\}} d_k^r = \operatorname{vol}(V)\left(\operatorname{vol}(V) - d_j^r\right) - d_1^r \\
&= \operatorname{vol}(V)\left(\operatorname{vol}(V) - 1\right) - d_1^r,
\end{aligned}$$

where $j \in V \setminus \{1\}$ in the second line. Hence, if $i \in V \setminus \{1\}$,

$$f_i^1 = 1 - \frac{\operatorname{vol}(V) - d_1^r}{\operatorname{vol}(V)} = \frac{d_1^r}{\operatorname{vol}(V)} > 0.$$

Furthermore, if $j \in V \setminus \{1\}$ and $i \in V \setminus \{j\}$,

$$f_i^j \geq \operatorname{vol}(V) - 1 - \frac{\operatorname{vol}(V)\left(\operatorname{vol}(V) - 1\right) - d_1^r}{\operatorname{vol}(V)} = \frac{d_1^r}{\operatorname{vol}(V)} > 0.$$

We conclude that $G \in \mathcal{C}$. □

Remark 7.2. The following is an example of a graph $G \in \mathcal{C}^0 \setminus \mathcal{C}$. Let G be the unweighted graph with $V = \{1, 2, 3, 4\}$ and $E = \{(1, 2), (2, 3), (3, 4)\}$. A quick computation verifies that the equilibrium measures $\nu^{V\setminus\{1\}}$ and $\nu^{V\setminus\{2\}}$ are given by, for $i \in V$,

$$\nu_i^{V\setminus\{1\}} := \begin{cases} 0, & \text{if } i = 1, \\ 2^{1+r} + 1, & \text{if } i = 2, \\ 2^{1+r} + 2^r + 2, & \text{if } i = 3, \\ 2^{1+r} + 2^r + 3, & \text{if } i = 4, \end{cases} \quad \text{and} \quad \nu_i^{V\setminus\{2\}} := \begin{cases} 1, & \text{if } i = 1, \\ 0, & \text{if } i = 2, \\ 2^r + 1, & \text{if } i = 3, \\ 2^r + 2, & \text{if } i = 4. \end{cases}$$

We also compute that

$$\operatorname{vol}(V) = 2^{r+1} + 2, \quad \mathcal{M}\left(\nu^{V\setminus\{1\}}\right) = 2^{2r+2} + 2^{r+2} + 2^{r+1} + 2^{2r} + 3, \quad \mathcal{M}\left(\nu^{V\setminus\{2\}}\right) = 2^{r+1} + 2^{2r} + 3.$$

Hence $\mathcal{A}\left(\nu^{V\setminus\{1\}}\right)_2 = 2^{r+1} + 1 + \frac{2^{2r}+1}{2^{r+1}+2} > \nu_2^{V\setminus\{1\}}$ and $\operatorname{vol}(V)\,\nu_1^{V\setminus\{2\}} = 2^r + 2 < 3 + 2^{r+1} < \mathcal{M}\left(\nu^{V\setminus\{2\}}\right)$, so $f_2^1 < 0$ and $f_1^2 < 0$ and thus $G \notin \mathcal{C}$. However, $(2^r + 1)(2^{r+1} + 2) = 2(2^{2r} + 2^{r+1} + 1) > 2^{2r} + 1$, and thus $\mathcal{A}\left(\nu^{V\setminus\{1\}}\right)_3 - 2^{r+1} - 1 = \frac{2^{2r}+1}{2^{r+1}+2} < \nu_3^{V\setminus\{1\}} - 2^{r+1} - 1$ and $\operatorname{vol}(V)\,\nu_3^{V\setminus\{2\}} = 2^{r+1} + 2^{2r} + 2^r + 2 > 2^{r+1} + 2^{2r} + 1 + 2 = \mathcal{M}\left(\nu^{V\setminus\{2\}}\right)$. Therefore $f_3^1 > 0$ and $f_3^2 > 0$. Since $\nu_4^{V\setminus\{1\}} > \nu_3^{V\setminus\{1\}}$ and $\nu_3^{V\setminus\{2\}} > \nu_3^{V\setminus\{2\}}$, it follows that also $f_4^1 > 0$ and $f_4^2 > 0$. The corresponding inequalities for f^3 and f^4 follow by symmetry. We conclude that, if $\omega_{ij} = 0$, then $f_i^j > 0$. Hence $G \in \mathcal{C}^0$.

Lemma 7.3. *Let $G = (V, E, \omega) \in \mathcal{G}$. For all $j \in V$, let $\nu^{V\setminus\{j\}}$ be the equilibrium measure which solves (M12) for $S = V \setminus \{j\}$ and define, for $i, j \in V$,*

$$\mathcal{N}_s(i, j) := \sum_{k\in\mathcal{N}(j)} \omega_{ik}, \tag{6}$$

where $\mathcal{N}(j)$ is the set of neighbours of node j, as in (M1) in the main paper. Then following statements are true.

1. *If, for all* $j \in V$ *and for all* $i \in \mathcal{N}(j)$, $\omega_{ij}\mathcal{M}\left(\nu^{V\setminus\{j\}}\right) \leq \operatorname{vol}(V)\, d_i^r$, *then* $G \in \mathcal{C}$.

2. *If, for all* $j \in V$ *and for all* $i \in V \setminus (\{j\} \cup \mathcal{N}(j))$, $\mathcal{N}_s(i,j)\mathcal{M}\left(\nu^{V\setminus\{j\}}\right) \leq \operatorname{vol}(V)\, d_i^r$, *then* $G \in \mathcal{C}^0$.

Proof. To prove these statements, we fix $j \in V$ and use a similar approach as in the proof of Lemma M3.6 in the main paper with $x := \frac{\mathcal{M}\left(\nu^{V\setminus\{j\}}\right)}{\operatorname{vol}(V)}$. Note, for $i \in V \setminus \{j\}$, that $\nu_i^{V\setminus\{j\}} \geq x$ implies that $f_i^j \geq 0$, where f_i^j is as in (M69).

To prove 1, set $S := V \setminus \{j\}$. We compute, for $i \in S$, $(\kappa_S)_i = d_i^r \omega_{ij}$. Note that the inequality in the assumption in 1 trivially holds for all $i \in V \setminus \mathcal{N}(j)$. Hence, for all $i \in S$, $x\,(\kappa_S)_i \leq 1$. Repeating the argument in the proof of Lemma M3.6, we find that, for all $i \in S$, $\nu_i^{V\setminus\{j\}} \geq x$, hence $G \in \mathcal{C}$.

To prove 2, set $S := V \setminus (\{j\} \cup \mathcal{N}(j))$. Then we have, for $i \in S$, $(\kappa_S)_i = d_i^{-r} \sum_{k\in\{j\}\cup\mathcal{N}(j)} \omega_{ij} = d_i^{-r}\left(\mathcal{N}_s(i,j) + \omega_{ij}\right) = d_i^{-r}\mathcal{N}_s(i,j)$. Hence, by assumption, for all $i \in S$, $x\,(\kappa_S)_i \leq 1$. Repeating again the argument in the proof of Lemma M3.6, we find that, for all $i \in S$, $\nu_i^S \geq x$. By statement M4 in Lemma M3.2, we also know that $\nu^{V\setminus\{j\}} \geq \nu^S$. Hence $G \in \mathcal{C}$. □

Remark 7.4. Note that, for the quantity in (6) we have $\mathcal{N}_s(i,j) = \sum_{k\in\mathcal{N}(j)\cap\mathcal{N}(i)} \omega_{ik}$. Hence, if $G \in \mathcal{G}$ is an unweighted graph, then $\mathcal{N}_s(i,j) = \mathcal{N}_s(j,i)$ is the number of *shared neighbours* of nodes i and j, i.e. the number of nodes k for which both edges (i,k) and (j,k) exist in E. We also see that, for all $G \in \mathcal{G}$ and $i \in V$, $\mathcal{N}_s(i,i) = d_i$.

Corollary 7.5. *Let* $G = (V,E,\omega) \in \mathcal{G}$ *be complete (see Definition 6.1). Then* $G \in \mathcal{C}^0$.

Proof. Let $j \in V$. Because G is complete, $\mathcal{N}(j) = V \setminus \{j\}$ and thus $V \setminus (\{j\} \cup \mathcal{N}(j)) = \emptyset$. It follows, either directly from the definition of $\mathcal{C}^0$, or from condition 2 in Lemma 7.3, that $G \in \mathcal{C}^0$. □

Remark 7.6. Let us consider a simple example to illustrate the conditions from Lemma 7.3. Let $G \in \mathcal{G}$ be the graph with node set $V = \{1,2,3\}$, edge set $E = \{(1,2),(2,3),(3,1)\}$ and edge weights $\omega_{12} = \omega_{23} = 1$ and $\omega_{13} = \omega > 0$. We note right away that, since G is a complete graph, condition 2 in Lemma 7.3 is trivially satisfied (see Corollary 7.5).

We compute $d_1 = d_3 = 1+\omega$, $d_2 = 2$, $\operatorname{vol}(V) = 4+2\omega$. We can confirm via direct computation that the equilibrium measure $\nu^{V\setminus\{1\}}$ is given by, for $i \in V$,

$$\nu_i^{V\setminus\{1\}} = \frac{1}{3+2\omega}\begin{cases} 0, & \text{if } i = 1,\\ 2^r(1+\omega) + (1+\omega)^2, & \text{if } i = 2,\\ 2^r + 2(1+\omega)^r, & \text{if } i = 3. \end{cases}$$

Therefore

$$\begin{aligned}\mathcal{M}\left(\nu^{V\setminus\{1\}}\right) &= \frac{2^r\left(2^r(1+\omega) + (1+\omega)^r\right) + (1+\omega)^r\left(2^r + 2(1+\omega)^r\right)}{3+2\omega}\\ &= \frac{2^{2r}(1+\omega) + 2^{r+1}(1+\omega)^r + 2(1+\omega)^{2r}}{3+2\omega}.\end{aligned}$$

If we choose $\omega = 1$, it is a matter of straightforward computation to check that condition 1 from Lemma 7.3 is satisfied for $j = 1$. Since the graph is fully symmetric when $\omega = 1$, it then follows that the condition is also satisfied for $j \in \{2,3\}$.

On the other hand, a computation with $\omega = 7$ and $r = 0$, shows that $\omega\mathcal{M}\left(\nu^{V\setminus\{1\}}\right) > \operatorname{vol}(V)\, d_3^r$, thus this provides an example of a graph for which condition 2 is satisfied, but condition 1 is not. Note that by continuity of $(r,\omega) \mapsto \omega\mathcal{M}\left(\nu^{V\setminus\{1\}}\right) - \operatorname{vol}(V)\, d_3^r$, the same is true for values of (r,ω) close to $(0,7)$.

Theorem M6.9 in the main paper shows that for graphs in $\mathcal{C}_\gamma$ there is a graph transformation which turns L into the graph Laplacian on the transformed graph. Lemma 7.7 gives estimates on the difference in weights of the original and new graphs.

Lemma 7.7. *Let* $\gamma \geq 0$ *and* $G = (V,E,\omega) \in \mathcal{C}_\gamma$. *Let* L *be as defined in (M46) in the main paper for* G. *Let* λ_m *and* ϕ^m *be the eigenvalues and corresponding eigenfunctions of the graph Laplacian* Δ, *as in*

(M35), (M36), with parameter $r = 0$. Let $\tilde{\omega}$ be as in (M73). Then, for all $i, j \in V$ for which $i \neq j$, we have

$$\gamma\left(\frac{1}{2}\sum_{m=1}^{n-1}\frac{\left(\phi_i^m-\phi_j^m\right)^2}{\lambda_m}-\frac{1-n^{-1}}{\lambda_1}\right)\leq\tilde{\omega}_{ij}-\omega_{ij}\leq\gamma\left(\frac{1}{2}\sum_{m=1}^{n-1}\frac{\left(\phi_i^m-\phi_j^m\right)^2}{\lambda_m}-\frac{1-n^{-1}}{\lambda_{n-1}}\right).$$

Proof. Let $i, j \in V$ be such that $i \neq j$. Combining (M76) with (M70) and (M71), we obtain

$$\tilde{\omega}_{ij}-\omega_{ij}=\frac{\gamma}{n}f_i^j=-\varphi_i^j=-\gamma\sum_{m=1}^{n-1}\lambda_m^{-1}\phi_i^m\phi_j^m.$$

Note that the matrix which has (the vector representations of) ϕ^m $(m = 0, \ldots, n-1)$ as orthonormal columns also has orthonormal rows, hence (since $r = 0$) we have that $\sum_{m=0}^{n-1}(\phi_i^m)^2 = 1$. Thus

$$\sum_{m=1}^{n-1}\lambda_m^{-1}\left(\phi_i^m\right)^2\leq\lambda_1^{-1}\sum_{m=1}^{n-1}\left(\phi_i^m\right)^2=\lambda_1^{-1}\left(\sum_{m=0}^{n-1}\left(\phi_i^m\right)^2-n^{-1}\right)=\lambda_1^{-1}\left(1-n^{-1}\right)$$

and similarly

$$\sum_{m=1}^{n-1}\lambda_m^{-1}\left(\phi_i^m\right)^2\geq\lambda_{n-1}^{-1}\left(1-n^{-1}\right).$$

Since

$$-\sum_{m=1}^{n-1}\lambda_m^{-1}\phi_i^m\phi_j^m=\frac{1}{2}\sum_{m=1}^{n-1}\lambda_m^{-1}\left(\phi_i^m-\phi_j^m\right)^2-\frac{1}{2}\sum_{m=1}^{n-1}\lambda_m^{-1}\left[\left(\phi_i^m\right)^2+\left(\phi_j^m\right)^2\right],$$

the result follows. □

Remark 7.8. If $r = 0$ and $\gamma \geq 0$[4], Theorem M6.9 from the main paper tells us that the dynamics of (M47) on a graph $G = (V, E, \omega) \in \mathcal{C}_\gamma$ correspond to diffusion dynamics on a different graph $\tilde{G} = (V, \tilde{E}, \tilde{\omega}) \in \mathcal{G}$ with the same node set V, but a different edge set and different edge weights. Furthermore, from Lemma M6.8 it follows that $E \subset \tilde{E}$, so $\tilde{G}$ can gain edges compared to G, but not lose any. By the same lemma we know that, if $G \in \mathcal{C}$, any edges that already existed in G cannot have a lower weight in $\tilde{G}$ than they had in G. Equation (M76) quantifies the change in edge weight. Lemma 7.7 suggests (but does not prove) that the largest increase (in the case when $G \in \mathcal{C}$) in edge weight (including potentially creation of a new edge where there was none in G) occurs between nodes $i \in V$ and $j \in V$ for which $\sum_{m=1}^{n-1}\frac{1}{\lambda_m}\left(\phi_i^m-\phi_j^m\right)^2$ is large. If this suggestion is accurate and G is such that the eigenvalues λ_m rapidly increase with increasing m, then the main addition of edge weight going from G to $\tilde{G}$ happens between those nodes i and j for which $\left(\phi_i^1-\phi_j^1\right)^2$ is large (or for which $\sum_{m=1}^{k}\left(\phi_i^m-\phi_j^m\right)^2$ is large, if the eigenvalue λ_1 has multiplicity k).

In this context it is interesting to note that the second smallest eigenvalue (when $r = 0$), i.e. the smallest nonzero eigenvalue for a connected graph, is called the *algebraic connectivity* of the graph and the corresponding eigenfunction (or eigenvector) is called the[5] *Fiedler vector* [Fie73]. In [GB06, OBO13, OBO14] it is argued that a good strategy when attempting to add an edge to a graph such as to maximize the algebraic connectivity of the resulting graph, is to add the edge between those nodes whose corresponding values in the Fiedler vector have a large (absolute) difference. In other words, adding an edge between those nodes i and j for which $(\phi_i^1 - \phi_j^1)^2$ is largest, is a good heuristic for maximizing the algebraic connectivity of a graph (if the addition of one edge is allowed). Our discussion above thus suggests that in going from graph G to graph $\tilde{G}$, most weight is added to those edges which make the largest contribution to the algebraic connectivity of the graph.

[4] If $\gamma = 0$, Lemmma 7.7 tells us that $\tilde{\omega} = \omega$, as expected since $L = \Delta$ in that case.
[5] Assuming the eigenvalue is simple.

Remark 7.9. The discussion in Remark 7.8 can give a some high level intuition about the dynamics of the M(mcOKMBO) algorithm on graphs in $\mathcal{C}_\gamma$. These dynamics can be seen as a diffusion process on a new graph which differs from the original graph by having additional (or more highly weighted) edges (approximately) between those nodes whose values in the eigenfunctions corresponding to the smallest nonzero eigenvalues of Δ differ by a large amount. The mass conserving thresholding step in M(mcOKMBO) distributes all the available mass over those nodes which, in the ODE step, acquired the most mass through this diffusion process on the new graph. Thus, the available mass from the initial function v^0 is most likely[6] to end up (after one iteration) at those nodes that are more strongly connected (in the new graph) to the nodes in the support of v^0, than to nodes in the support's complement. These connections could have been present already in the original graph, or they could have been created (or strengthened) via the newly created edges determined in large part by the eigenfunctions (corresponding to the smallest nonzero eigenvalues) of Δ. The relative influence of both these effects is controlled by the parameter γ.

Lemma M6.11 in the main paper shows that sets $S \subset V$ which minimize $F_0(\chi_S)$ have to balance their 'volume', $\sum_{i\in S} \tilde{d}_i$, and curvature, $\sum_{i\in S} (\tilde{\kappa}_S)_i$, on the new graph $\tilde{G}$. We have put 'volume' in scare quotes here, because $\tilde{r} = 0$ in Lemma M6.11, thus $\sum_{j\in S} \tilde{d}_j$ is not equal to $\mathrm{vol}\,(S)$ on $\tilde{G}$.

In the following, we use the unweighted star graphs from Definition 6.1 to illustrate some of the concepts discussed so far in this section and in Section M6. Remember from Lemma 7.1 that these star graphs are in $\mathcal{C}$, so they are suitable examples.

Lemma 7.10. *Let $G \in \mathcal{G}$ be an unweighted star graph as in Definition 6.1 with $n \geq 3$ nodes. Then the functions $\varphi^1, \varphi^j : \mathcal{V} \to \mathbb{R}$, for $j \in V \setminus \{1\}$, as defined in (M70) in the main paper, are given by, for $i \in V$,*

$$\varphi_i^1 = (\mathrm{vol}\,(V))^{-2} \begin{cases} (n-1)^{r+1}, & \text{if } i = 1, \\ -(n-1)^{2r}, & \text{if } i \neq 1, \end{cases}$$

$$\varphi_i^j = (\mathrm{vol}\,(V))^{-2} \begin{cases} -(n-1)^r, & \text{if } i = 1, \\ ((n-1)^r + n - 1)^2 - 2(n-1)^r - (n-1), & \text{if } i = j, \\ -2(n-1)^r - (n-1), & \text{if } 1 \neq i \neq j. \end{cases}$$

Assume $r = 0$ and let $\gamma \geq 0$. Let $\tilde{\omega}$ be as in (M73), then, for $i, j \in V$,

$$\tilde{\omega}_{ij} = \begin{cases} 0, & \text{if } i = j, \\ 1 + \frac{\gamma}{n^2}, & \text{if } i = 1 \neq j \text{ or } j = 1 \neq i, \\ \frac{\gamma(n+1)}{n^2}, & \text{if } i \neq 1 \neq j \neq i. \end{cases}$$

Proof. A direct computation can be performed to validate that, for all $j \in V$, φ^j indeed solves (M45) for $\chi_{\{j\}}$, but we will give a different derivation here based directly on (M70) and (M69). Noting that $d_1 = n-1$ and, for $i \in V \setminus \{1\}$, $d_i = 1$, and using Lemma 6.5, we compute $\mathcal{M}\left(\nu^{V\setminus\{1\}}\right) = \sum_{i=2}^n d_i^r = n-1$ and, for $j \in V \setminus \{1\}$,

$$\mathcal{M}\left(\nu^{V\setminus\{j\}}\right) = d_1^r(\mathrm{vol}\,(V) - 1) + \sum_{i\in V\setminus\{1,j\}} d_i^r \mathrm{vol}\,(V) = (\mathrm{vol}\,(V))^2 - 2\mathrm{vol}\,(V) + n - 1.$$

Furthermore, $\frac{d_1^r}{\mathrm{vol}(V)} = 1 - \frac{n-1}{\mathrm{vol}(V)}$ and, for $j \in V \setminus \{1\}$, $\frac{d_j^r}{\mathrm{vol}(V)} = \frac{1}{\mathrm{vol}(V)}$. Combining these results with the expressions for $\nu^{V\setminus\{1\}}$ and $\nu^{V\setminus\{j\}}$ in Lemma 6.5, we find that φ^1 and φ^j are as defined in this lemma.

Now assume that $r = 0$ and let $i, j \in V$. Per definition, if $i = j$, then $\tilde{\omega}_{ij} = 0$. If $i \neq j$, we know, by (M76) and (M70), that $\tilde{\omega}_{ij} = \omega_{ij} + \frac{\gamma}{n} f_i^j = \omega_{ij} - \varphi_i^j$. A direct computation for $r = 0$ shows that, for $j \in V \setminus \{1\}$, $i \in V$,

$$\varphi_i^1 := \begin{cases} \frac{n-1}{n^2}, & \text{if } i = 1, \\ -\frac{1}{n^2}, & \text{if } i \neq 1, \end{cases} \qquad \varphi_i^j := \begin{cases} -\frac{1}{n^2}, & \text{if } i = 1, \\ \frac{n^2-n-1}{n^2}, & \text{if } i = j, \\ -\frac{n+1}{n^2}, & \text{if } 1 \neq i \neq j. \end{cases} \tag{7}$$

[6] This should currently be interpreted as an imprecise, nonrigorous, statement, but might be turned into a precise conjecture for future research.

Note that for all $i, j \in V$, $\varphi_i^j = \varphi_j^i$, as should be the case per Corollary M6.6. The result now follows from the fact that for all $j \neq 1$, $\omega_{1j} = 1$ and all other ω_{ij} are 0. □

Remark 7.11. In the proof of Lemma 7.10 we computed the functions φ^j, for $j \in V$, using the equilibrium measures from Lemma 6.5. It is instructive to compute φ^j directly from the eigenvalues and eigenfunctions as well, for the case $r = 0$. Using Lemma 6.8, we see that, for $i, j \in V$,

$$\varphi_i^j = \sum_{m=1}^{n-2} \phi_i^m \phi_j^m + \frac{1}{n} \phi_i^{n-1} \phi_j^{n-1}. \tag{8}$$

In Section 10.4 we give the details showing that this computation leads to the same expression for φ^j as given above in (7).

Remark 7.12. If we want to apply the observation from Remark 7.8 to the star graphs discussed above, we see from Lemma 6.8 that the smallest nonzero eigenvalue is 1 with multiplicity $n-2$. Hence, from Remark 7.8, we expect that $\tilde{\omega}_{ij} - \omega_{ij}$ is largest for those nodes i, j for which $\sum_{m=1}^{n-2} \left(\phi_i^m - \phi_j^m\right)^2$ is large[7]. From Lemma 6.8 we have, for $m \in \{1, \ldots, n-2\}$ and $i \in V$,

$$\begin{aligned}
(\phi_i^m)^2 &= \frac{(n-i)^2}{(n-i)^2 + n - i}(1-\delta_{i1})(1-\delta_{in}) + (1-\delta_{i1})(1-\delta_{i2}) \sum_{m=1}^{i-2} \frac{1}{(n-m-1)^2 + n - m - 1}, \\
&= \frac{n-i}{n-i-1}(1-\delta_{i1})(1-\delta_{in}) + \frac{i-2}{(n-i+1)(n-1)}(1-\delta_{i1})(1-\delta_{i2}),
\end{aligned}$$

where we used the Kronecker delta and (15). Furthermore, if $m \in \{1, \ldots, n-2\}$ and $i, j \in V$ with $j < i$, then

$$\begin{aligned}
\phi_i^m \phi_j^m &= -\frac{n-j}{(n-j)^2 + n - j} + (1-\delta_{j1})(1-\delta_{j2}) \sum_{m=1}^{j-2} \frac{1}{(n-m-1)^2 + n - m - 1} \\
&= \frac{1}{n-j+1} + (1-\delta_{j1})(1-\delta_{j2}) \frac{j-2}{(n-j+1)(n-1)}.
\end{aligned}$$

Hence, for $j < i$,

$$\begin{aligned}
&\sum_{m=1}^{n-2} \left(\phi_i^m - \phi_j^m\right)^2 = \sum_{m=1}^{n-2} \left((\phi_i)^2 + (\phi_j)^2 - 2\phi_i \phi_j\right) \\
&= \begin{cases}
\frac{n-i}{n-i+1} + \frac{i-2}{(n-i+1)(n-1)} + \frac{2}{n}, & \text{if } j = 1 \text{ and } i \neq n, \\
\frac{n-2}{n-1} + \frac{2}{n}, & \text{if } j = 1 \text{ and } i = n, \\
\frac{n-i}{n-i+1} + \frac{i-2}{(n-i+1)(n-1)} + \frac{n-j}{n-j+1} + \frac{j-2}{(n-j+1)(n-1)} + \frac{2}{n-j+1} - \frac{2(j-2)}{(n-j+1)(n-1)}, & \text{if } j \neq 1 \text{ and } i \neq n, \\
\frac{n-2}{n-1} + \frac{n-j}{n-j+1} + \frac{j-2}{(n-j+1)(n-1)} + \frac{2}{n-j+1} - \frac{2(j-2)}{(n-j+1)(n-1)}, & \text{if } j \neq 1 \text{ and } i = n,
\end{cases} \\
&= \begin{cases}
\frac{n^2-2}{n(n-1)}, & \text{if } j = 1 \text{ and } i \neq n, \\
\frac{n^2-2}{n(n-1)}, & \text{if } j = 1 \text{ and } i = n, \\
2, & \text{if } j \neq 1 \text{ and } i \neq n, \\
2, & \text{if } j \neq 1 \text{ and } i = n.
\end{cases}
\end{aligned}$$

The second equality follows by straightforward simplification of the fractions. The case where $j > i$ follows by symmetry.

There are two things we can immediately note. First, despite there being an apparent difference in computation of the cases $1 \neq i \neq n$ and $1 \neq i = n$, there is of course no difference in eventual outcome.

[7] Unfortunately, while the star graph has served us very well in previous examples, it is not the cleanest case to illustrate our heuristic from Remark 7.8. The symmetry of the star graph, which has simplified some of the calculations in earlier examples, now means that our heuristic requires some more calculation, since we cannot suffice with checking $\left(\phi_i^1 - \phi_j^1\right)^2$ only.

As we expect by symmetry of the star graph, each of the nodes $\{2,\dots,n\}$ is interchangable without affecting the outcome. Most importantly for our present purposes, we have that $\frac{n^2-2}{n(n-1)} < 2$. In fact, a direct calculation shows that $\frac{n^2-2}{n(n-1)}$ has a maximum value of $\frac{7}{6}$ for $n \in \{n \in \mathbb{N} : n \geq 2\}$, which is attained at $n = 3$ and $n = 4$. Hence, according to our heuristic, the increase $\tilde{\omega} - \omega$ between the leaves (i.e. nodes $\{2,\dots,n\}$) of the star graph should be larger than the incease between the leaves and the centre node 1. This is indeed what we saw in Lemma 7.10.

8 Pinning for $\mathcal{C}_\gamma$ and for M(mcOKMBO)

The following pinning bound for graphs in $\mathcal{C}_\gamma$ uses Corollary M6.16.

Lemma 8.1. *Let $\gamma \geq 0$ and let $G = (V, E, \omega) \in \mathcal{C}_\gamma$. Let $S \subset V$ be nonempty and define*

$$\tau_\kappa(S) := \frac{1}{2}\|L\chi_S\|^{-1}_{\mathcal{V},\infty}.$$

Let S^1 be the first set in the corresponding M(OKMBO) evolution of the initial set $S^0 = S$. If $0 \leq \tau < \tau_\kappa(S)$, then $S^1 = S$.

Proof. The proof is based on (parts of the) proof of [vGGOB14, Theorem 4.2].

Writing the solution $u(t) = e^{-tL}\chi_S$ to (M47) at $t = \tau$ as $u(\tau) = \chi_S - \int_0^\tau L(u(t))\,dt$, we find

$$\begin{aligned}\|u(\tau) - \chi_S\|_{\mathcal{V},\infty} &\leq \int_0^\tau \|L(u(t))\|_{\mathcal{V},\infty}\,dt \leq \int_0^\tau \|e^{-tL}L\chi_S\|_{\mathcal{V},\infty}\,dt \leq \int_0^\tau \|L\chi_S\|_{\mathcal{V},\infty}\,dt \\ &= \tau\|L\chi_S\|_{\mathcal{V},\infty} < \frac{1}{2},\end{aligned}$$

where we used that L and e^{-tL} commute for the second inequality, and Corollary M6.16 for the third inequality. We conclude that $S^1 = S$. □

Remark 8.2. In Lemma 5.10 and Remark 5.11 we see that if τ is chosen too small in M(OKMBO) pinning occurs, while if τ is chosen too large, a constant stationary state will be achieved in one iteration of M(OKMBO). The choice of τ is also critically important for M(mcOKMBO), yet the details of the situation are somewhat different in this case.

Using the expansion in (M57), which expresses the solution to (M47) in terms of the eigenvalues and eigenfunctions from Lemma M5.8 in the main paper, we see that $u(t) \to \mathcal{A}(u_0)$ as $t \to \infty$. Thus for large τ, the function $u(\tau) \in \mathcal{V}$ will be approximately constant. It will typically not be exactly constant though, and hence the mass conserving threshold step of M(mcOKMBO) could still be able to produce a non-arbitrary result, in the sense that the result is based on an actual ordering inherent in $u(\tau)$ instead of on an arbitrary ordering of nodes on all of which $u(\tau)$ has the same value. However, for those nodes $i, j \in V$ for which $u_i(\tau) \neq u_j(\tau)$, the differences in value of $u(\tau)$ are likely very small when τ is large. In a numerical implementation they might even be below machine precision, which renders the resulting output meaningless, determined by the particularities of the sorting algorithm used, instead of the mathematical problem. From Section M5.2 in the main paper we know that, for F_0 minimization purposes, we are mainly interested in small τ, so we will avoid choosing τ too large in our implementations in Sections M7 and 9.

When τ is small, pinning can occur in the M(mcOKMBO) algorithm[8], as it did in M(OKMBO), but the underlying reasons are different in both cases. In M(OKMBO) pinning at a node occurs when τ is so small that the value of u at that node changes by an amount less than (or equal to) $1/2$, whereas pinning in M(mcOKMBO) occurs in step k, if, for all $i, j \in V$ for which $v_i^{k-1} = 1 \neq v_j^{k-1}$ we have $\left(e^{-\tau L}v^{k-1}\right)_i > \left(e^{-\tau L}v^{k-1}\right)_j$, and for all $i, j \in V$ for which $v_i^{k-1} = 0 \neq v_j^{k-1}$ we have $\left(e^{-\tau L}v^{k-1}\right)_i < \left(e^{-\tau L}v^{k-1}\right)_j$[9]. We

[8] We say that pinning occurs in the k^{th} step if $v^k = v^{k-1}$.

[9] Pinning definitely occurs if these two strict inequalities hold. Depending on which choices the ordering process makes when there are $i, j \in V$ for which $v_i^{k-1} = v_j^{k-1}$, pinning might also occur if non-strict inequalities hold instead. For simplicity of the discussion we assume that the ordering process is such that if in step $k-1$ node i is ranked before node j, then these nodes retain their relative ordering in step k unless $v_i^k < v_j^k$ (in particular, we assume their relative ordering does not change if $v_i^k = v_j^k$).

need both these conditions to guarantee that $v^k = v^{k-1}$, because of the possibility that v^{k-1} or v^k take values in $(0,1)$ at a single node. In a situation where v^{k-1} and v^k are guaranteed to be in $\mathcal{V}_M^b$, e.g. when $r = 0$, and v^{k-1} is not constant we can simplify these pinning conditions: pinning will not occur if

$$\min_{i\in\{i\in V: v_i^{k-1}=1\}} \left(e^{-\tau L}v^{k-1}\right)_i < \max_{j\in\{j\in V: v_j^{k-1}=0\}} \left(e^{-\tau L}v^{k-1}\right)_j . \tag{9}$$

When v^{k-1} and v^k are not guaranteed to be in $\mathcal{V}_M^b$, the condition above is still sufficient, but might not be necessary, for the absence of pinning.

9 Numerical implementations

9.1 Example graphs

For the purpose of having visually appealing results, in the experiments we present here we have mostly used graphs whose structure resembles a discretization of the plane —such as the graphs G_{torus}, G_{stitched}, and even, to a degree, G_{moons}, which are introduced below— as they allow us to see pattern formation similar to what we expect based on the continuum case [vG08, Chapter 2]. For example, spherical droplets (Figure 6a) or lamellar patterns (Figure 6b). However, the algorithm is not restricted to such examples; in the visually less interesting examples we will still display the evolution of the value of F_0 along the sequence of M(mcOKMBO) iterates, to illustrate that the algorithm does (mostly) decrease the value of F_0 also in these cases. In this paper we present results obtained on the following graphs:

- An unweighted 4-regular graph (i.e. each node has degree 4) which can be graphically represented as the grid obtained by tessellating a square with periodic boundary conditions (i.e. the square two-dimensional flat torus) with square tiles, see for example Figure 5[10]. We denote this graph by $G_{\text{torus}}(n)$, where n is the number of nodes (and thus $\sqrt{n}$ is the number of nodes along each direction of the square in the tesselation representation).

- An unweighted graph obtained by adjoining a square lattice graph (this time without periodic boundary conditions) and a triangular lattice graph, as in Figure 4 (see also [vGGOB14]. We will denote these 'stitched together' graphs by $G_{\text{stitched}}(n)$ where n is the total number of nodes in the graph.

- A two moon graph constructed as in [BH09]. This graph is constructed by sampling points from two half-circles in $\mathbb{R}^2$, embedding these into a high-dimensional space, adding Gaussian noise, and constructing a weighted K-nearest neighbour graph with the sample points represented by the nodes. We will denote this graph by G_{moons}. It has 600 nodes. See Figures M1 and M2 in the main paper.

- To illustrate that the method can also be applied to more complex networks, we use a symmetrized version of the weighted "neural network" graph obtained from [New] and based on [WSTB86, WS98]. It represents the neural network of C. Elegans and has 297 nodes. Since the original network with weight matrix A is directed, we use the symmetrized weight matrix $\frac{1}{2}(A + A^T)$. We will denote the resulting undirected, weighted, graph by G_{neural}. See Figure 2.

9.2 Choice of τ

The choice of τ is an important one. We know from the discussion in Remark 8.2 that τ should not be chosen too small or too large, but it is not easy to decide a priori what a good choice would be. The discussion in Remark M5.16 in the main paper suggests that, if minimizing F_0 in (M34) (with $q = 1$) is our goal, then we should choose τ small, but the potential for pinning prevents us from choosing τ too small. It is also worthwhile to note that, while the Γ-convergence results in Section M5.2 in the

[10] In order to increase the visibility of the patterns in the function values on the nodes, the size of the nodes as depicted was chosen to be large. As a consequence, in the figure the nodes cover the edges and the edges are no longer visible; for each node edges are present between it and each of the four nodes placed immediately adjacent to it, taking into account periodic boundary conditions.

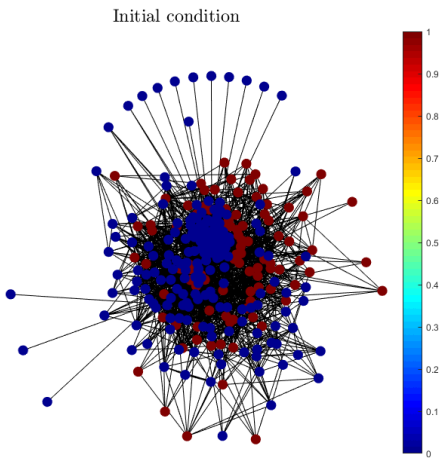

(a) Initial condition

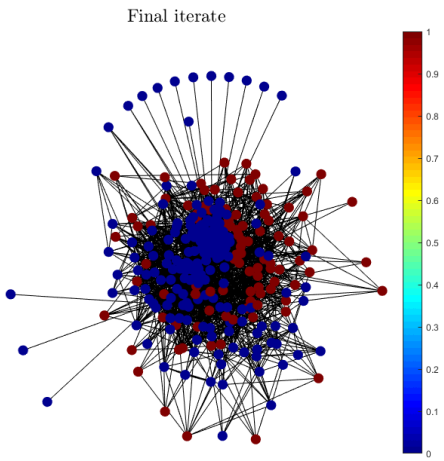

(b) Final iterate ($k = 2$)

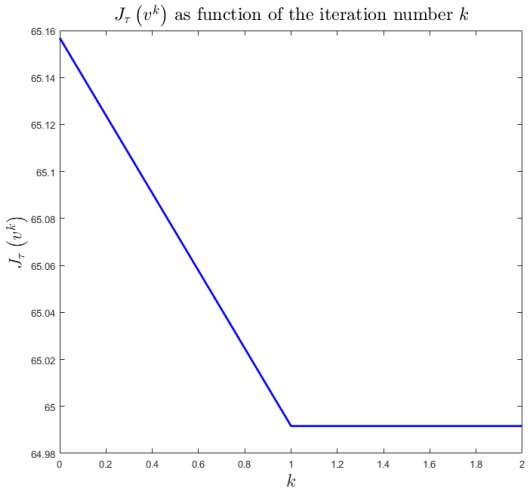

(c) Plot of $J_{0.75}\left(v^k\right)$

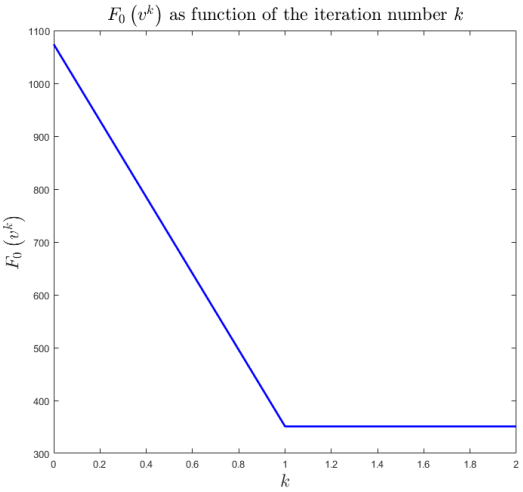

(d) Plot of $F_0\left(v^k\right)$

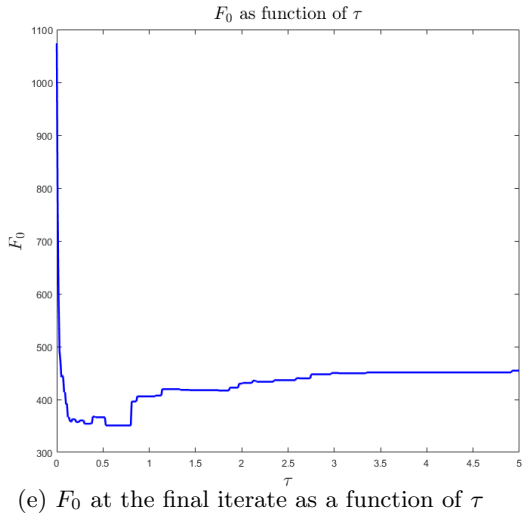

(e) F_0 at the final iterate as a function of τ

Figure 2: Results from Algorithm M(mcOKMBO) on G_{neural} with $r = 0$, $\gamma = 1$, and $M = 100$. The initial condition in Figure 2a was constructed using option (b) in Section 9.3 and was used to obtain the other results displayed here. The results in Figures 2b, 2c, and 2d were obtained for $\tau = 0.75$, in which case the value of F_0 at the final iterate is approximately 350.95. The graph in Figure 2e shows the values of F_0 at the final iterates for a ranges of values of τ, with a resolution on the τ axis (step size) of 0.01.

main paper guarantee convergence of minimizers of J_τ over $\mathcal{K}_M$ to a minimizer of F_0 over $\mathcal{V}_M^b$, there is no monotonicity result in the sense that we do not know if minimizers of J_τ for smaller τ are better approximations.

One might think that the condition in (9) (for v^0) gives us some guidance in choosing τ. After all, we do not want the algorithm to pin straight away in the first iteration. There are, however, some difficulties with this approach. The condition does not give us a way to determine τ a priori, before actually computing $e^{-\tau L}v^0$, and so while it might serve as a condition to reject or accept a given τ a posteriori (which boils down to being a glorified trial and error approach), it does not directly help in deciding on τ beforehand. We experimented with replacing the exponentials in (9) with their linear or quadratic Taylor approximations at $\tau = 0$. While such approximations allow us to find a value of τ which satisfies the approximated version of the inequality (9), in our experiments these τ did not satisfy the exact inequality.

Even if we do manage to find a τ which satisfies the condition in (9) for v^0, this same τ might not satisfy the condition for v^1 or some other v^{k-1} down the line. In fact, we know that M(mcOKMBO) does terminate, hence there is a k for which τ violates the condition for v^{k-1}. It is not at all clear which k is the preferred final iteration number, even if we could somehow design a way to choose τ at the start in such a way to have the algorithm terminate after this preferred k^{th} iteration. Lemma M5.18 tells us that J_τ decreases along iterates of the M(mcOKMBO) algorithm, but it does not tell us how close each iterate is to minimizing J_τ.

We did consider (and experimented with) updating τ in each iteration of M(mcOKMBO) such that it satisfies (9) with v^{k-1} in the k^{th} iteration. This might seem a good approach, but it does not actually address the problems described above and introduces some new ones. First of all, we are still posed with the same difficulties we had in choosing a good τ based on v^0, only now at each iteration. Second, this introduces the question of when to stop updating τ. If we update τ after each iteration such that it satisfies (9) in each new iteration, the algorithm will only terminate once it reaches a state in which (9) has no solutions, which is not necessarily guaranteed to be a preferred state. One possible choice could be to terminate when the only possible choices lead to a new value of τ that is higher than the previous value of τ (with some possible leeway in the first few iterations, to allow the scheme to move away from the initial condition). Third, such iterative updating of τ introduces a new layer of difficulty in the theoretical interpretation of the algorithm. If we run M(mcOKMBO) at a fixed τ, we know that we do so in order to minimize J_τ (even though we do not know how well the final iterate approximates a minimzer), which in turn we do because such minimizers approximate minimizers of J_τ (by Theorem M5.13 in the main paper). Updating τ in each step complicates the first part of that interpretation.

In our experiments the results obtained by updating τ did not outperform results obtained with fixed τ (measured by the value of F_0 at the final iterate). It might be that significant improvements can be obtained with the right update rule (we tried various ad hoc update techniques that would allow the algorithm to progress through a number of iterations before terminating), but since we did not discover such rule if it even exists, in this paper all the results we present are obtained with fixed τ, chosen by trial and error. The graphs and results in Figures 3, 8, and 11 show how the final value of F_0 obtained by the algorithm can vary greatly depending on the choice of τ. Note that large values of τ can lead to spurious patterns as explained in more detail in Section 9.5.

In Figure 3 we see detailed results obtained at two different values of τ with all the other parameter values kept the same. The resulting final iterates in Figures 3a and 3b are very different. The latter has a significantly lower value of F_0 than the former (228.42 versus 454.96) and is thus a better approximation of a minimizer of F_0. It is however not an exact minimizer, as in this case we can obtain even lower values of F_0 by choosing a different initial condition (namely the one in Figure 5b, as is explained in more detail in Section 9.3 and can be seen in Figures 6a and 6e.

In most of the numerical results we present here, F_0 decreases monotonically along the sequence of M(mcOKMBO) iterates (until the penultimate iterate after which it stays constant; see the discussion of the stopping criterion in Section 9.4). Figure 8f shows that this is not always the case. In Figures 4d and M2d (the latter in the main paper) we even see cases in which the value of F_0 at the final iterate is higher than at some of the earlier iterates. If the required additional memory and computation time are available, at every iteration of M(mcOKMBO) one can store the state which has obtained the lowest value of F_0 so far and use that state as approximate minimizer of F_0 upon termination of the algorithm. Note, however, from Figures 8d, 4c, and M2c (the latter in the main paper) that also in those cases the value of J_τ does decrease along the sequence of iterates, as it is guaranteed to do by Lemma M5.18.

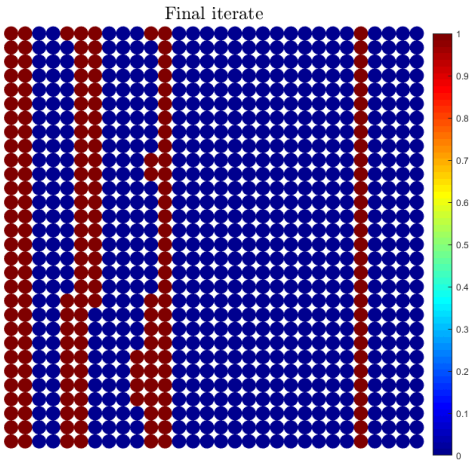

(a) Final iterate ($k = 3$) for $\tau = 1$

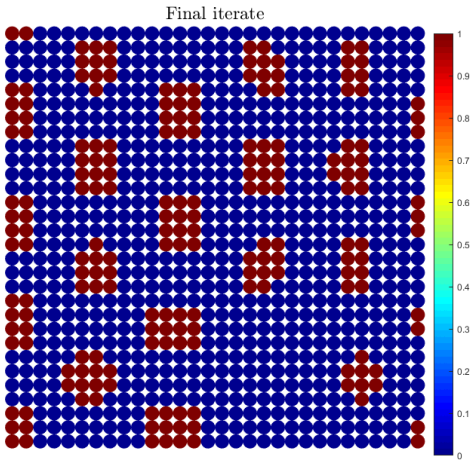

(b) Final iterate ($k = 13$) for $\tau = 5$

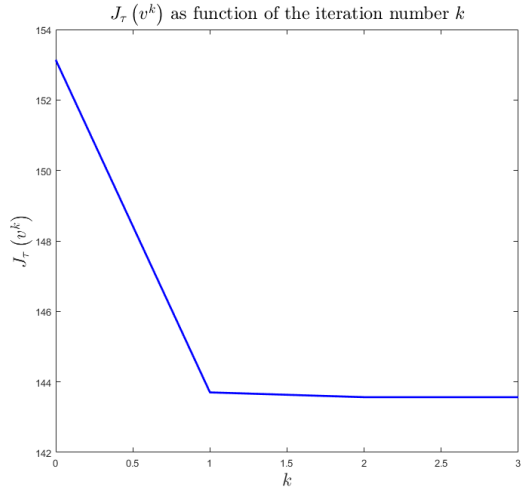

(c) Plot of $J_1\left(v^k\right)$

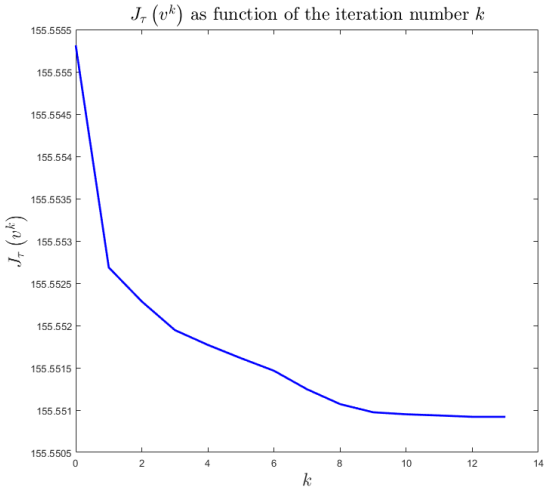

(d) Plot of $J_5\left(v^k\right)$

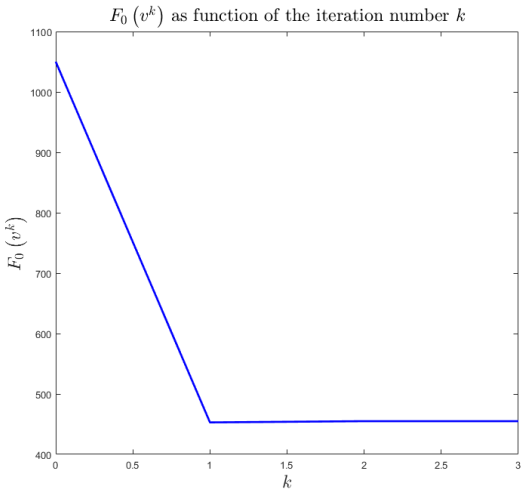

(e) Plot of $F_0\left(v^k\right)$ for $\tau = 1$

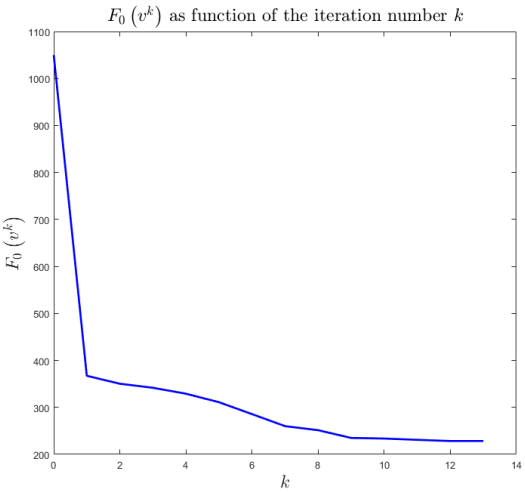

(f) Plot of $F_0\left(v^k\right)$ for $\tau = 5$

Figure 3: Results from Algorithm M(mcOKMBO) on $G_{\text{torus}}(900)$ with $r = 0$, $\gamma = 1$, and $M = 200$. The initial condition from Figure 5a was used. The figures in the left column were obtained with $\tau = 1$, the ones on the right with $\tau = 5$. The value of F_0 at the final iterate is approximately 454.96 for $\tau = 1$ and 228.42 for $\tau = 5$.

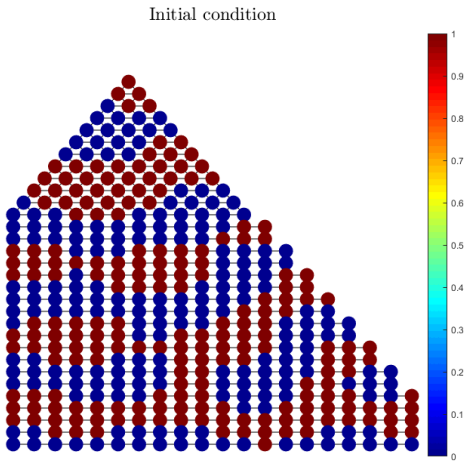

(a) Initial condition

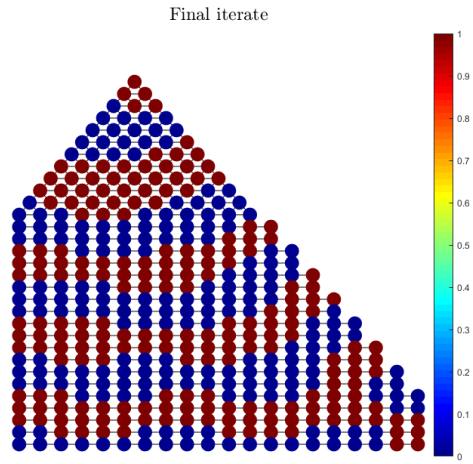

(b) Final iterate ($k = 8$)

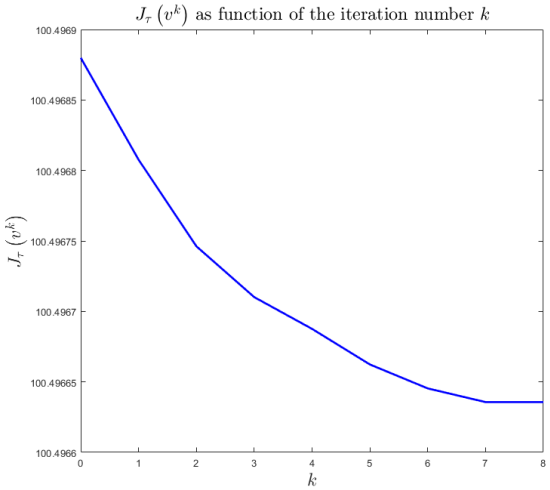

(c) Plot of $J_5\left(v^k\right)$

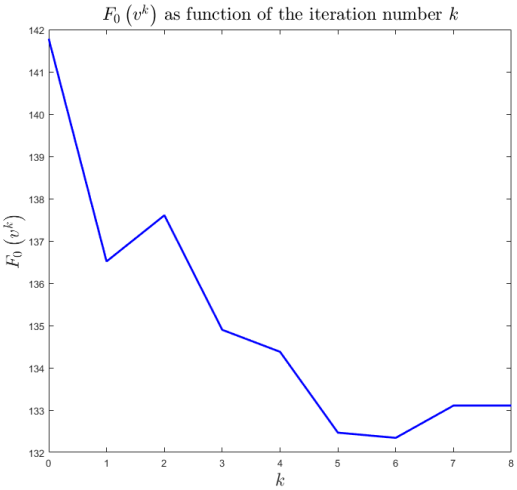

(d) Plot of $F_0\left(v^k\right)$

Figure 4: Results from Algorithm M(mcOKMBO) on $G_{\text{stitched}}(402)$ with $r = 0$, $\gamma = 1$, $M = 201$, and $\tau = 5$. The initial condition in Figure 4a was constructed according to option (c) in Section 9.3. The value of F_0 at the final iterate is approximately 133.11.

9.3 Choice of initial condition

Up until now, we have not paid much attention to the choice of initial condition, but in practice this choice has a big influence on the final state of M(mcOKMBO); different initial conditions can lead to final states with significantly different values of F_0. In the experiments which we report on here[11] we used three different options for constructing initial conditions:

(a) Assign the available mass to random nodes (by applying the mass conserving thresholding step of M(mcOKMBO) to a random vector generated by MATLAB's `rand` function). A realization of such a randomly constructed initial condition is given in Figure 7b.

(b) Cluster the initial mass together in one part of the graph. This description is necessarily somewhat vague, as it is not a well-defined method in itself which is applicable across all choices of graphs. Instead, in this option we let the structure of the graph suggest the structure of the initial condition. It is best illustrated by specific examples, e.g. assigning all mass to the nodes in one strip of the square grid/discretized torus or one part of the stitched mess; see Figures 5a and 7a. Figure 2a shows another example where this option was used[12].

(c) Construct v^0 based on the eigenfunctions ϕ^m by applying the mass conserving thresholding step to an eigenvector ϕ^m corresponding to the smallest nonzero eigenvalue of L[13]. When this eigenvalue Λ_m has multiplicity greater than 1, the choice of ϕ_m is not unique (besides the 'standard' non-uniqueness in sign when $m \geq 1$). In our experiments we choose ϕ_m to be the sum of all eigenfunctions (after normalization) that MATLAB's `eig` function returns corresponding to Λ_m[14]. Examples of initial conditions constructed in this way are given in Figures 5b, 5c, 5d, M1a, M1c, and M1e (the latter three in the main paper). It should be noted that, while some of these initial conditions are very close to the final iterate they lead to, they are not (in our experiments that are presented here) equal to the final iterates. Even in those cases in which the initial condition is closest to the final iterate (out of the cases we present here), i.e. those in Figure 6, the algorithm goes through at least one iteration before arriving at the final state. That is not to say the algorithm cannot pin (it will of course, if τ is chosen small enough), but it shows that the eigenfunctions are not necessarily stationary states of the algorithm and M(mcOKMBO) can improve on those states.

Comparing the right column of Figure 3 with the left column of Figure 6 we see a case in which the eigenfunction based initial condition (option (c) above) gives better results than the 'structured' approach of option (b) with all other parameters kept the same. The latter (Figure 3) gives a final value of F_0 of approximately 228.42, whereas the former gives a value of approximately 206.59. Option (c) is not always preferred though. In Figures 7 and 8 we see that both the value obtained with the initial condition in Figure 7b (which is a particular realization of the random process of option (a)) and the value obtained with the initial condition from Figure 7a (option (b)) are both lower than the value obtained with option (c) (Figure 5d), with all other parameters kept the same: 102.01 and 122.83, respectively, versus 126.05. We can improve the result obtained with option (c) by choosing a different τ ($\tau = 7$ instead of $\tau = 5$ in Figures 8b and 8f), but the resulting value 104.01 is still higher than the lowest value in Figure 7 (at $\tau = 7$ options (a) and (b) did perform worse than option (c) in our experiments; not pictured). We did not find any τ values that achieved lower F_0 values in this case. It should also be noted that of course not every realization of the random process that generates the initial condition in option (a) achieves the same low value for F_0. In a separate run of 10 experiments (which did not include the run pictured

[11] We also tried some other initial conditions in $\mathcal{K}_M \setminus \mathcal{V}_M^{ab}$, $\mathcal{K} \setminus \mathcal{V}^b$, and $\mathcal{V}^b \setminus \mathcal{V}_M^b$, such as states with the mass spread out evenly over all nodes or other constant functions, states with randomly spread mass (which differs from option (a) described in the main text of Section 9.3 in that this state is usually not binary), and states constructed by changing a function $\mathcal{V}_M^{ab}$ at one node to make it binary. In our test these approaches were never optimal, so we will not spend more time on them here.

[12] In practice this is achieved by applying the mass conserving threshold step to the vector $(n, n-1, \ldots, 1)^T$, where the numbering of the nodes in G_{torus} and G_{stitched} is clear from the resulting initial conditions in Figures 5a and 7a, respectively, and the node numbering in G_{neural} is the one inherited from the dataset from [New].

[13] Other variations we tried include using other eigenvalues, e.g. the smallest non-zero eigenvalue of Δ, (since, for small γ, we can view L as a perturbation of Δ in the sense of Theorem M6.9 in the main paper), and applying the mass conserving threshold step to the vector with entries $\left|\pm\phi_i^m\right|$ (or $\pm\left|\sum_m \phi_i^m\right|$ in the case of a non-simple eigenvalue) to reflect (in crude approximation) the fact that the relevant quantity to minimize in (M44) is $\left|\langle v^0, \phi^m\rangle_{\mathcal{V}}\right|$. None of those choices stood out from option (c) mentioned in the main text of Section 9.3.

[14] Note that this still could be machine dependent, as `eig` does not necessarily use a consistent order.

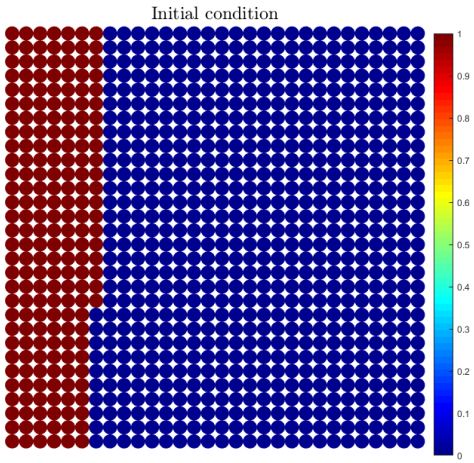

(a) 'Structured' initial condition

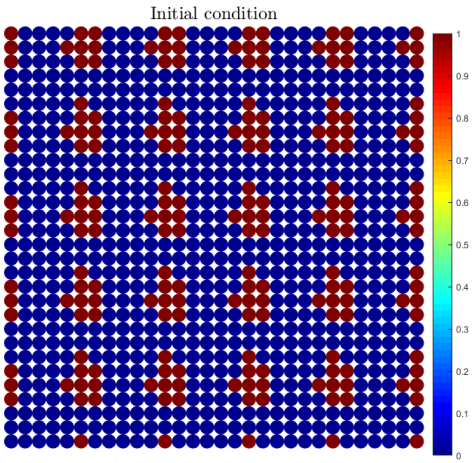

(b) Eigenfunction based initial condition

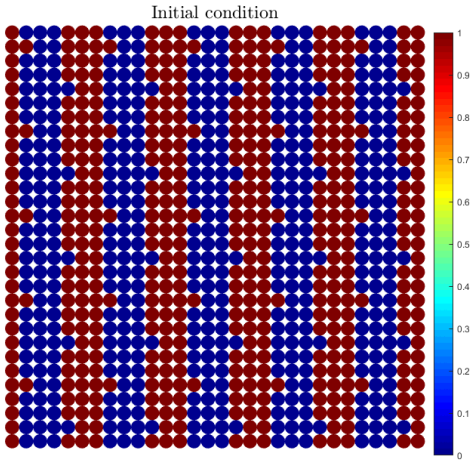

(c) Eigenfunction based initial condition

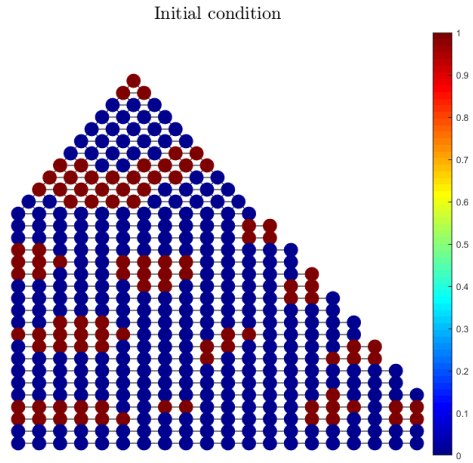

(d) Eigenfunction based initial condition

Figure 5: Three different initial conditions for M(mcOKMBO) on $G_{\text{torus}}(900)$ and one on $G_{\text{stitched}}(402)$, all with $r = 0$. The top two figures have $M = 200$, the bottom left figure has $M = 450$, the bottom right one $M = 201$. The initial condition in the top left figure is 'structured' in the sense of option (b) in Section 9.3; the others are based on eigenfunctions as in option (c) in Section 9.3.

in the right column of Figure 7, but used the exact same parameters) we obtained an average final value for F_0 of 118.77 with a (corrected sample) standard deviation (obtained via `std` in MATLAB) of 26.84, a maximum of 191.24 and a minimum of 101.84 (all numbers rounded to two decimals).

For some non-optimal initial conditions, we see patterns emerge that look like the intermediate-time phase ordering pictures in [Ito98, Figure 2], as we see in Figure 9. Figure 10 has been constructed using the same parameter choices as Figure 9, but uses an initial condition constructed using option (b), instead of an eigenfunction based initial condition (option (c)). In this case a lower final value of F_0 is achieved.

9.4 Other choices in the problem setting and the algorithm

There are some other choices to make, besides the graph, τ, and the initial condition, before running the M(mcOKMBO) algorithm, both in the set-up of the original problem (M34) as well as for the algorithm.

The parameter γ is a parameter that is part of the original problem setting (M34). Its value does not only influence the structure of the (approximate) solutions, but also influences what the appropriate choices of τ and v^0 are. As, for given $m \neq 0$, $\gamma \mapsto \Lambda_m$ is an increa-sing function and τ always appears in

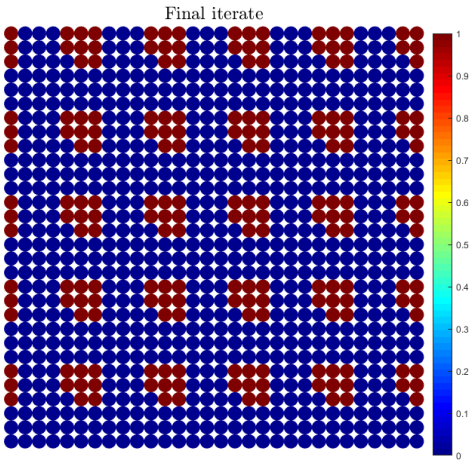

(a) Final iterate ($k = 3$) for $M = 200$

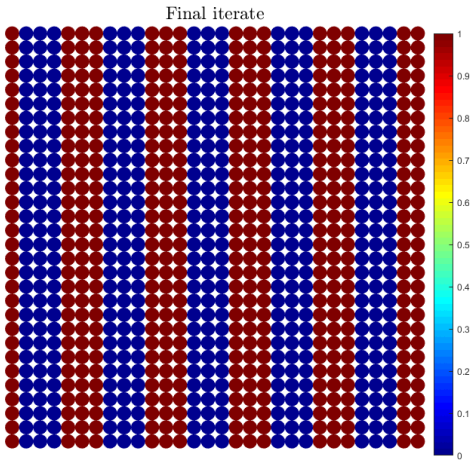

(b) Final iterate ($k = 2$) for $M = 450$

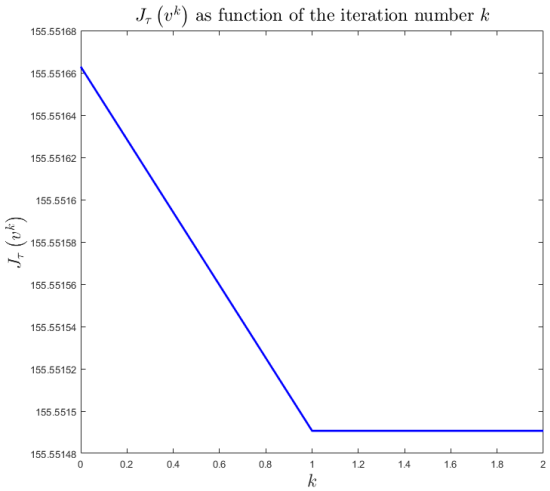

(c) Plot of $J_5\left(v^k\right)$

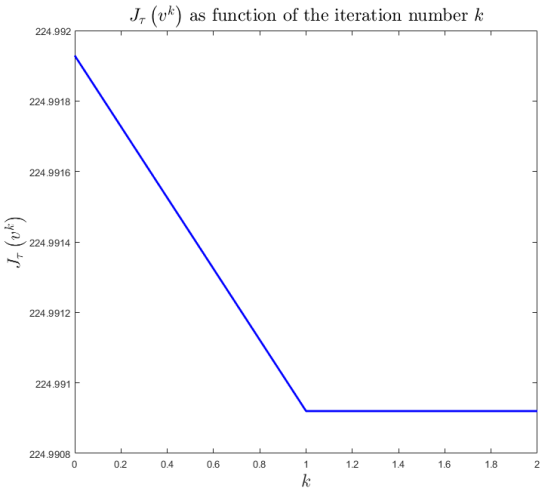

(d) Plot of $J_5\left(v^k\right)$

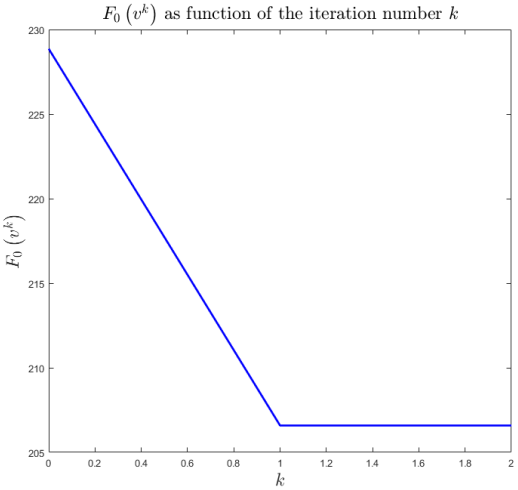

(e) Plot of $F_0\left(v^k\right)$ for $M = 200$

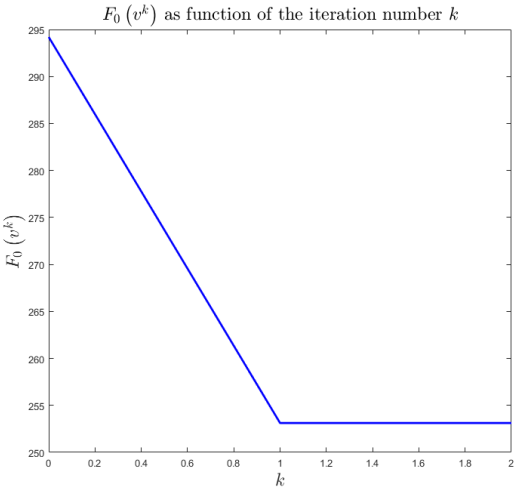

(f) Plot of $F_0\left(v^k\right)$ for $M = 450$

Figure 6: Results from Algorithm M(mcOKMBO) on $G_{\text{torus}}(900)$ with $r = 0$, $\gamma = 1$, and $\tau = 5$. The figures in the left column were obtained with $M = 200$ and the initial condition from Figure 5b, the ones on the right with $M = 450$ and the initial condition from Figure 5c. The value of F_0 at the final iterate is approximately 206.59 for $M = 200$ and 253.12 for $M = 450$.

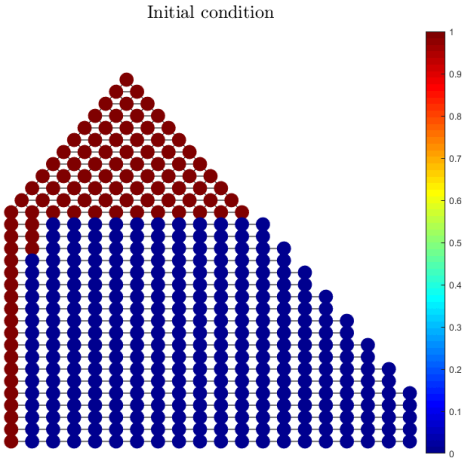

(a) Initial condition

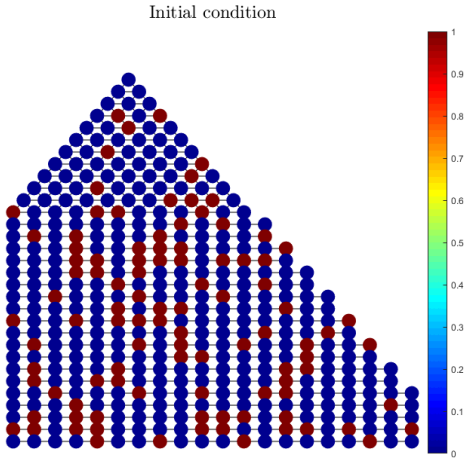

(b) Initial condition

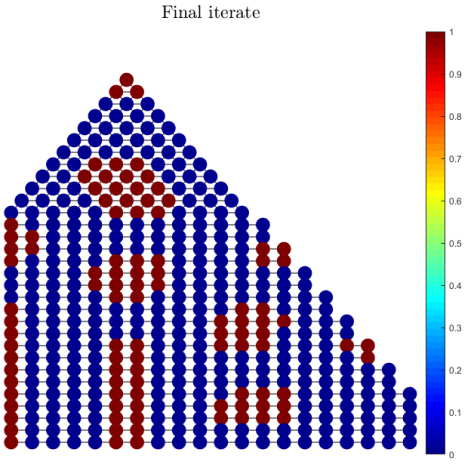

(c) Final iterate ($k = 13$) starting from Fig. 7a

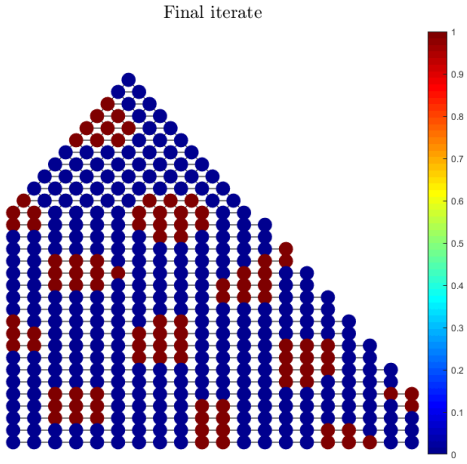

(d) Final iterate ($k = 9$) starting from Fig. 7b

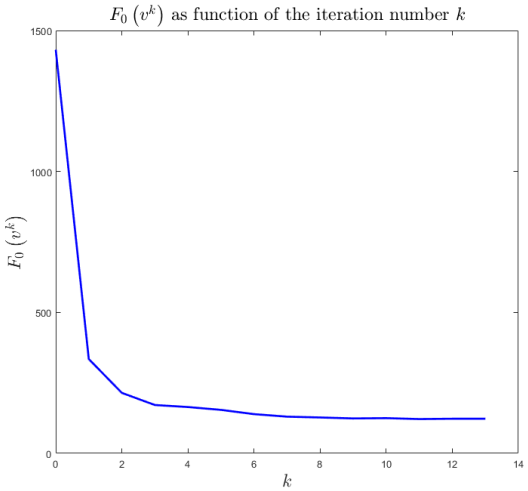

(e) Plot of $F_0\left(v^k\right)$ starting from Fig. 7a

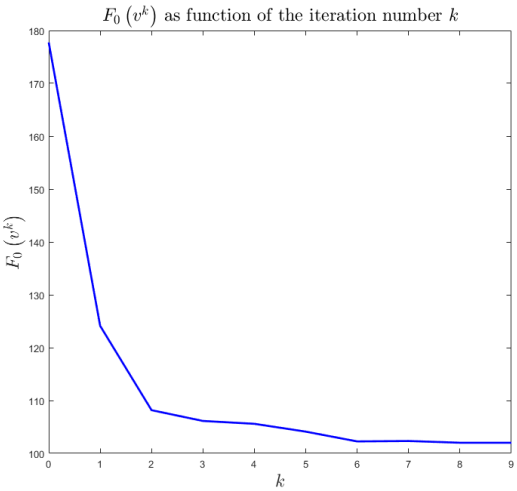

(f) Plot of $F_0\left(v^k\right)$ starting from Fig. 7b

Figure 7: Results from Algorithm M(mcOKMBO) on $G_{\text{stitched}}(402)$ with $r = 0$, $\gamma = 1$, $M = 100$, and $\tau = 5$. The left and right columns correspond to the cases in which the initial conditions from Figures 7a (option (b) from Section 9.3) and 7b (option (a)), respectively, were used. The value of F_0 at the final iterate is approximately 122.83 on the left and 102.01 on the right.

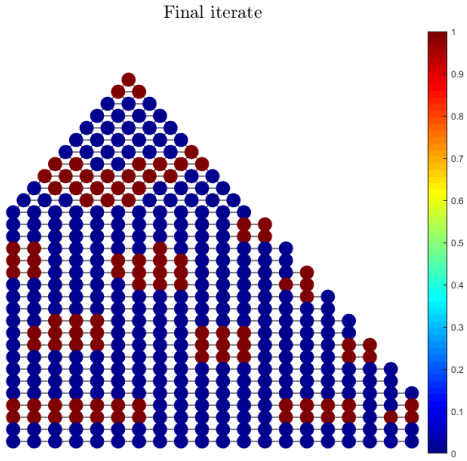

(a) Final iterate ($k = 4$) with $\tau = 5$

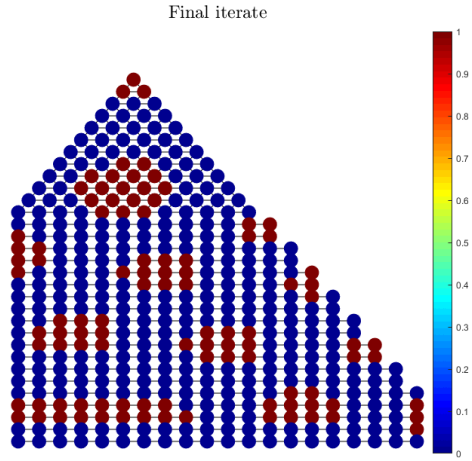

(b) Final iterate ($k = 9$) with $\tau = 7$

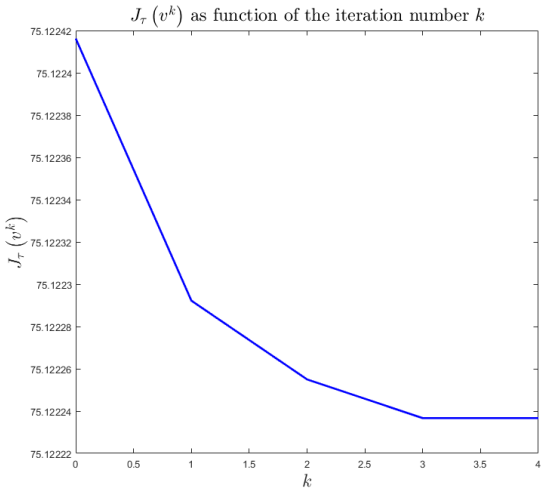

(c) Plot of $J_5\left(v^k\right)$ with $\tau = 5$

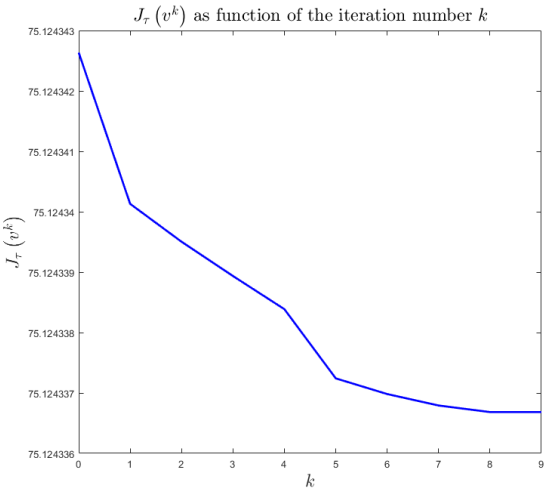

(d) Plot of $J_7\left(v^k\right)$ with $\tau = 7$

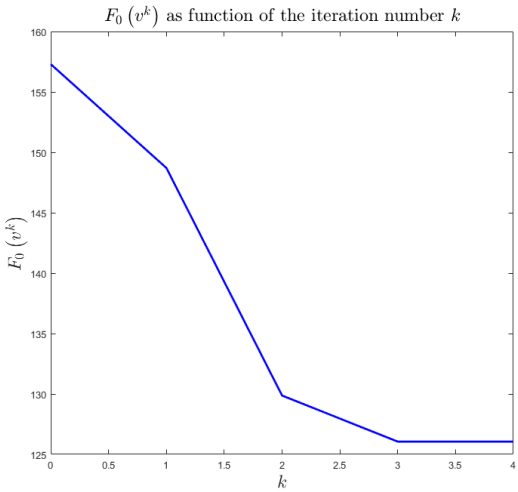

(e) Plot of $F_0\left(v^k\right)$ with $\tau = 5$

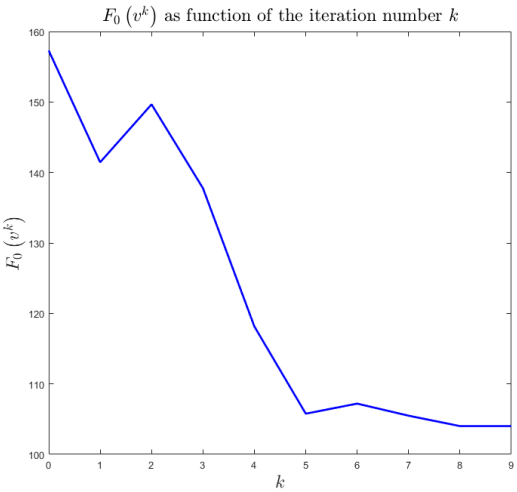

(f) Plot of $F_0\left(v^k\right)$ with $\tau = 7$

Figure 8: Results from Algorithm M(mcOKMBO) on $G_{\text{stitched}}(402)$ with $r = 0$, $\gamma = 1$ and $M = 100$ and starting from the initial condition in Figure 5d. The left and right columns in the two lower rows correspond to the cases in which $\tau = 5$ and $\tau = 7$, respectively. The value of F_0 at the final iterate is approximately 126.05 on the left and 104.01 on the right.

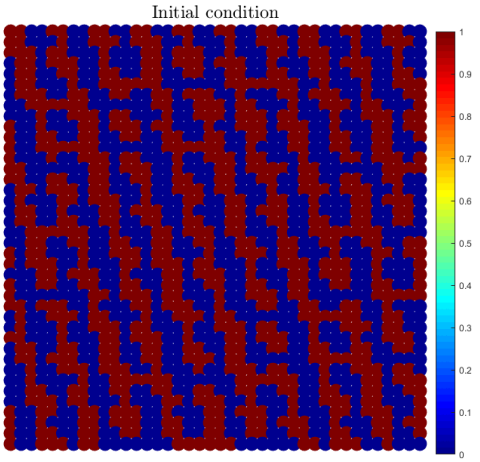

(a) Initial condition

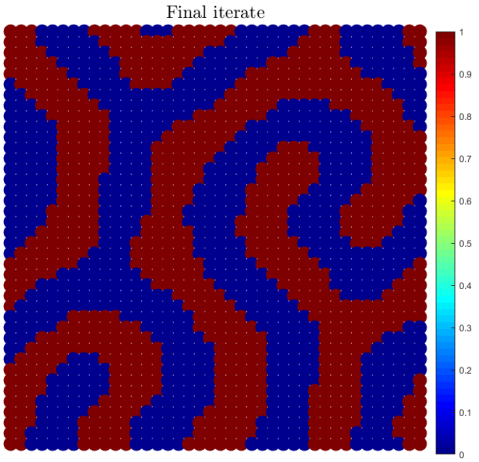

(b) Final iterate ($k = 25$)

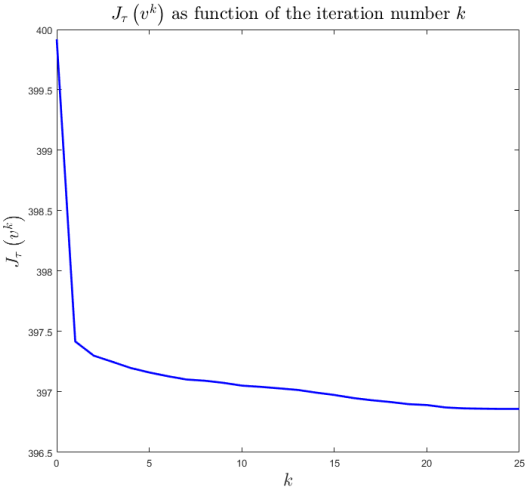

(c) Plot of $J_5\left(v^k\right)$

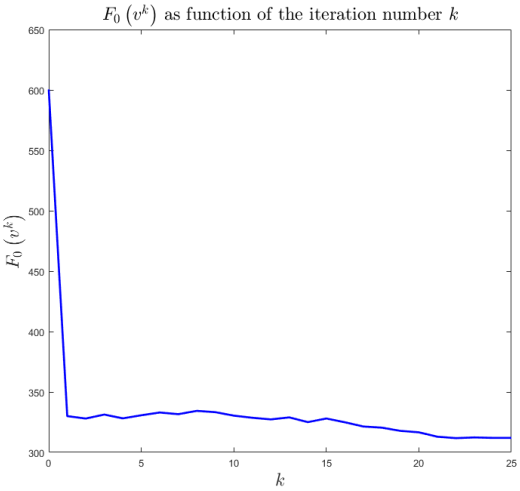

(d) Plot of $F_0\left(v^k\right)$

Figure 9: Results from Algorithm M(mcOKMBO) on $G_{\text{torus}}(1600)$ with $r = 0$, $\gamma = 0.2$, $M = 800$, and $\tau = 5$. The initial condition in Figure 9a was constructed using option (c) in Section 9.3 and was used to obtain the other results displayed here. The value of F_0 at the final iterate is approximately 311.99.

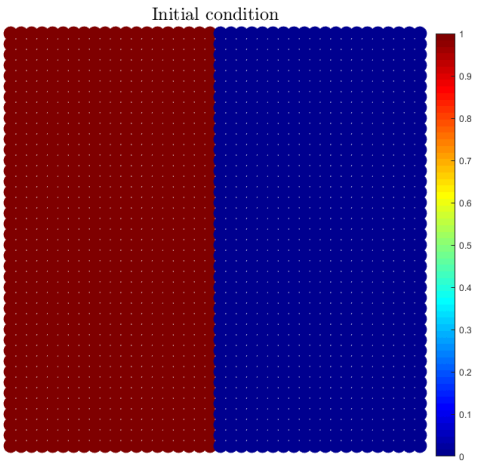

(a) Initial condition

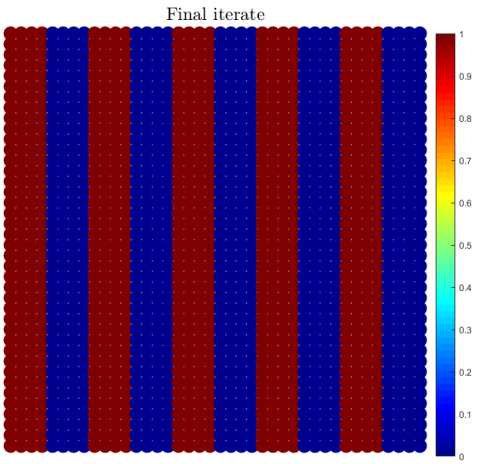

(b) Final iterate ($k = 3$)

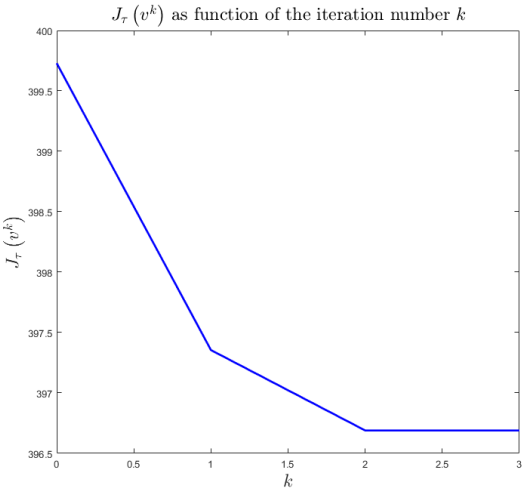

(c) Plot of $J_5\left(v^k\right)$

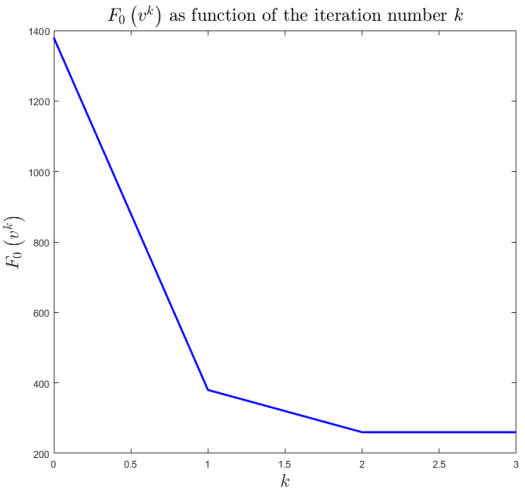

(d) Plot of $F_0\left(v^k\right)$

Figure 10: Results from Algorithm M(mcOKMBO) on $G_{\text{torus}}(1600)$ with $r = 0$, $\gamma = 0.2$, $M = 800$, and $\tau = 5$. The initial condition in Figure 10a was constructed using option (b) in Section 9.3 and was used to obtain the other results displayed here. The value of F_0 at the final iterate is 260.

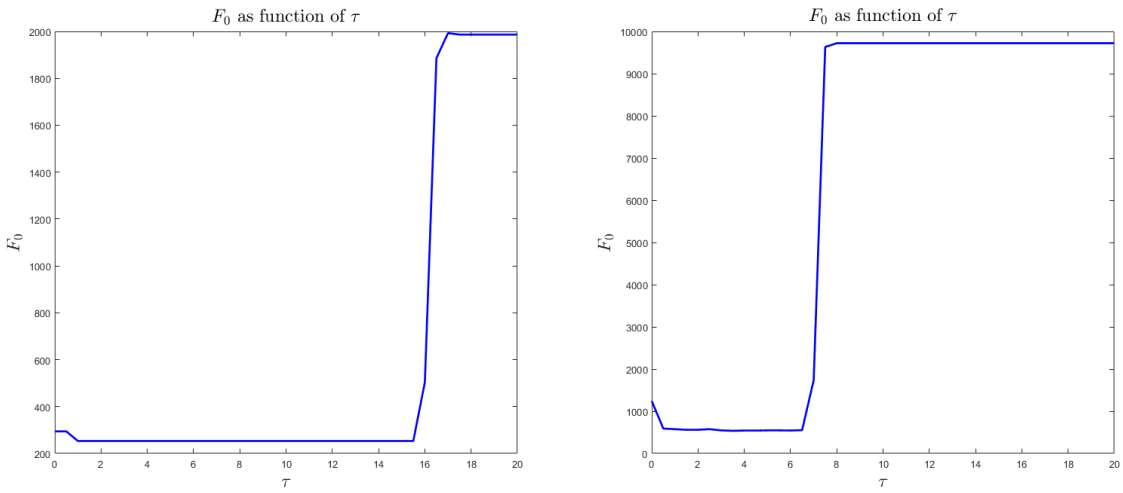

(a) $\gamma = 1$ (b) $\gamma = 5$

Figure 11: The value of $F_0\left(v^k\right)$, where v^k is the final iterate of M(mcOKMBO), as a function of τ, for two different values of γ. In both cases $G_{\text{torus}}(900)$ was used, with $r = 0$, $M = 450$, and the initial condition from Figure 5c. The resolution on the τ axis (step size) is 0.5 for both graphs.

the combination $\tau\Lambda_m$ in the algorithm via (M57), increasing γ decreases the values of τ at which good results are obtained (all other things being equal). We see an example of this in Figure 11. The choice of γ also has an influence on the order of the eigenvalues Λ_m, as per Remark 5.5, hence the eigenfunction based method for choosing v^0 described in Section 9.3 (option (c)) is also influenced by the choice of γ.

The parameters r and q, that are part of the original setup of our function spaces $\mathcal{V}$ and $\mathcal{E}$ also play a role. The value of q changes the value of F_0. Important results, such as Corollary M4.12 and Theorem M5.13 in the main paper, have been obtained under the assumption that $q = 1$, hence that is also the choice we make when we compute the value of F_0 for our experiments. Note however that the choice of q does not influence the actual algorithm M(mcOKMBO).

The choice of r does influence the problem setup in (M34) and the algorithm M(mcOKMBO). The functional F_0 is independent of r, but the mass functional $\mathcal{M}$ is not. As noted a few times in other places (e.g. in Sections M2 and M5.3 of the main paper), when $r \neq 0$ the mass condition can be very restrictive in that the set $\mathcal{V}_M^b$ (or even $\mathcal{V}_M^{ab}$) can be very small. This is especially the case if the graph has a highly irregular degree distribution. Hence all the examples we show are for the case $r = 0$. The parameter r also influences M(mcOKMBO) through its effect on Δ.

Different prescribed masses M can lead to different patterns in the final state. For example, in Figure 6 we see that (in that example, with, in particular $r = 0$) $M = 200$ leads to a droplet pattern, while the larger mass $M = 450$ leads to a lamellar pattern. This is in line with what is expected based on the continuum case [vG08, Chapter 2].

Finally we mention N, the number of iterations in M(mcOKMBO) (or M(OKMBO)). Up until now we have assumed that the algorithm is run for a preset number of iterations, mostly for notational convenience; we know, however, that the algorithm converges in a finite number of steps, in the sense which was made precise in Lemma M5.18 (or Corollary M5.5) in the main paper. It thus makes sense to add a stopping criterion to the algorithm. In our experiments we set $N = 500$ and add a stopping criterion which ends the algorithm's run if the Euclidean norm of the difference between (the vector representations of) v^{k-1} and v^k is less than 10^{-24}. This tolerance in practice means that the algorithm stops before it has run through 500 iterations if and only if $v^k = v^{k-1}$. In fact, in our examples the algorithm runs for at most a few dozen iterations before the stopping criterion kicks in and never gets to the (arbitrarily chosen) maximum of 500 iterations. Note that as a consequence, in all our examples the states obtained in the final two iterations are the same. For example, in the left hand column of Figure 3 the final value of k is 3. Hence $v^3 = v^2$ and in that case the algorithm only took two iterates to arrive at its final state. In the right hand side of that same figure the algorithm took twelve iterates to arrive at the final state $v^{12} = v^{13}$.

9.5 Spurious patterns

Because mass is conserved in M(mcOKMBO) and the iterates of the algorithm are forced to be in $\mathcal{V}_M^{ab}$, patterns are guaranteed to appear, in the sense that mass will be allocated to some nodes and not to others, giving the appearance of a pattern. We used MATLAB's `sort` function to produce the relabelling R_u in the mass conserving threshold step of M(mcOKMBO). This function will produce an output, even if u has the same value on two or more nodes. This means that our choice of sorting method, effectively hides the non-uniqueness that is inherent in the choice of R_u when u takes the same value at different nodes. This is desirable when the non-uniqueness involves the relabelling of a small number of nodes only, since some choice of R_u has to be made to continue the algorithm and the influence of that choice on the final state (and value of F_0) is presumably small in that case. However, when u has the same value on many different nodes (within machine precision), for example when τ in the ODE step has been chosen too large, the resulting non-uniqueness in the choice of R_u is very large (e.g. for constant u all relabelling functions R_u are equally admissible). Hence the resulting output of the mass conserving threshold step is (close to) arbitrary, yet it will still produce a pattern when visualized. Thus it is important to have a way to identify if this has occurred or if the resulting pattern is indeed meaningful in the context of the F_0 minimization problem of (M34).

One could inspect the function u before the mass conserving threshold step and discard the result if u is (too close to being) constant. The problem with this approach is that it is not a priori clear what "too close to" means. In our experiments sometimes the variation in node values of u (as measured by the standard deviation, computed with MATLAB's `std` function) is on the order of 10^{-12} (or less) and yet still meaningful in the sense explained below.

Luckily we have an arbiter of meaning in this case. After all, our goal is to minimize F_0, hence as long as F_0 decreases along the iterates of M(mcOKMBO) the algorithm (and thus also the mass conserving threshold step) is performing a meaningful operation. A decrease in the values of the functional J_τ can also be used to justify confidence in the output of the algorithm. We include plots of the values of F_0 and F_τ as function of the iteration number k with our results in this paper to validate the algorithm's ouput.

10 Deferred proofs and computations

10.1 Proof of Lemma M3.2

These results are proven in [BCE03, Section 2] for $r = 0$. The same proofs, mutatis mutandis, work for general $r \in [0, 1]$. Because the equilibrium measures play an important role in the current paper, however, we will provide our own proofs here, which deviate slightly from those in [BCE03, Section 2] in places.

To prove the statements in item M1, we note that, by identity (M2), for all $u \in V$, $\langle \Delta u, u\rangle_{\mathcal{V}} = \|\nabla u\|_{\mathcal{E}}^2 \geq 0$ and thus Δ is positive semidefinite on $\mathcal{V}$. Moreover, equality is achieved if and only if $\nabla u = 0$. Because G is connected $\nabla u = 0$ if and only if u is constant. If $u \in \mathcal{V}_0$ then u is constant if and only if $u = 0$. Hence, if $u \in \mathcal{V}_0$ and $u \neq 0$, then $\|\nabla u\|_{\mathcal{E}}^2 > 0$ and thus Δ is positive definite on $\mathcal{V}_0$.

To prove statement M2, let $u \in \mathcal{V}_+$. We first observe that the result follows trivially if $\operatorname{supp}(u) = V$. Hence we now assume that $\operatorname{supp}(u) \neq V$. If $j \in V \setminus \operatorname{supp}(u)$, then $(\Delta u)_j = -d_j^{-r} \sum_{k\in V} \omega_{jk} u_k \leq 0$. Hence $\max_{i\in V\setminus\operatorname{supp}(u)}(\Delta u)_i \leq 0$. Now let $l \in \operatorname{supp}(u)$ be such that, for all $k \in \operatorname{supp}(u)$, $u_l \geq u_k$. Then $(\Delta u)_l = d_l^{-r} \sum_{k\in V} \omega_{lk}(u_l - u_k) \geq d_l^{-r} \sum_{k\in V\setminus\operatorname{supp}(u)} \omega_{lk}(u_l - u_k) \geq 0$. Hence $\max_{i\in\operatorname{supp}(u)}(\Delta u)_i \geq 0 \geq \max_{i\in V\setminus\operatorname{supp}(u)}(\Delta u)_i$ and the result follows.

Let S be a proper subset of V. To prove the uniqueness claim in M3, assume that $\nu_1^S, \nu_2^S \in \mathcal{V}_+$ are both solutions of (M12). Define $\nu := \nu_1^S - \nu_2^S$, then $\Delta\nu = 0$ on S and $\nu = 0$ on S^c. Let $V' = S$ and apply Lemma M3.1 twice, once with $u = \nu$, $v = 0$ and once with $u = 0$, $v = \nu$. This shows that $\nu = 0$ and thus $\nu_1^S = \nu_2^S$.

Next we show that (M12) has a solution in $\mathcal{V}_+$. Let S be a proper subset of V. Alll norms on finite dimensional vector spaces are topologically equivalent and if we interpret $u \mapsto \frac{1}{2}\|\nabla u\|_{\mathcal{E}}^2$ as a function from the Euclidean space $\mathbb{R}^n$ to $\mathbb{R}$, it is continuous (being a polynomial in n variables). Hence it is also continuous as a functional on $\mathcal{V}$. The set $\mathcal{V}_{+,1}(S) := \{u \in \mathcal{V}_+ \cap \mathcal{V}_1 : \operatorname{supp}(u) \subset S\}$ interpreted as subset of $\mathbb{R}^n$ is closed and bounded and thus compact. Hence it is also compact as subset of $\mathcal{V}$. Thus there is a

$u^* \in \mathcal{V}_{+,1}(S)$ such that, for all $u \in \mathcal{V}_{+,1}(S)$, $\frac{1}{2}\|\nabla u^*\|_{\mathcal{E}}^2 \le \frac{1}{2}\|\nabla u\|_{\mathcal{E}}^2$. In other words, u^* is the solution to the minimization problem

$$\begin{aligned}&\min_{u\in V} \frac{1}{2}\|\nabla u\|_{\mathcal{E}}^2\\ &\text{subject to } \forall i \in V\ u_i \ge 0, \quad \forall j \in V\setminus S\ u_j = 0, \quad \text{and} \quad \mathcal{M}(u) = 1.\end{aligned}$$

Thus u^* satisfies the Karush-Kuhn-Tucker (KKT) optimality conditions [BV04, Section 5.5.3] [NW99, Theorem 12.1] for this minimization problem, which give us the existence of $\chi_1 : V \to [0,\infty)$, $\chi_2 : V\setminus S \to \mathbb{R}$, and $\chi_3 \in \mathbb{R}$, such that, for all $i \in V$ and all $j \in V\setminus S$,

$$\begin{aligned} d_i^r\left(\Delta u^*\right)_i - \sum_{k\in V}\left(\chi_1\right)_k \delta_{ik} + \sum_{k\in V\setminus S}\left(\chi_2\right)_k \delta_{ik} + \chi_3 d_k^r = 0, \\ u_i^* \ge 0, \quad \left(\chi_1\right)_i \ge 0, \quad \left(\chi_1\right)_i u_i^* = 0, \\ u_j^* = 0, \quad \mathcal{M}\left(u^*\right) = 1.\end{aligned} \tag{10}$$

Hence

$$\begin{aligned}0 &= \sum_{k\in V}\left(\chi_1\right)_k u_k^* = \sum_{k\in S}\left(\chi_1\right)_k u_k^* = \sum_{k\in S} d_k^r\left(\left(\Delta u^*\right)_k + \chi_3\right) u_k^* \\ &= \sum_{k\in V} d_k^r\left(\left(\Delta u^*\right)_k + \chi_3\right) u_k^* = \langle \Delta u^*, u^*\rangle_{\mathcal{V}} + \chi_3 \mathcal{M}\left(u^*\right).\end{aligned}$$

Thus, using (M2), we find $\chi_3 = -\|\nabla u^*\|_{\mathcal{E}}^2$.

Assume $i \in S$ and $u_i^* = 0$, then $\left(\chi_1\right)_i > 0$. Moreover, $d_i^r\left(\Delta u^*\right)_i = -d_i^r \sum_{k\in V}\omega_{ik}u_k \le 0$ and $\chi_3 d_i^r = -d_i^r\|\nabla u^*\|_{\mathcal{E}}^2 \le 0$. Hence, by the first KKT condition above in (10), $-\left(\chi_1\right)_i \ge 0$, which is a contradiction. Hence, if $i \in S$, then $u_i^* > 0$. In that case the KKT conditions give $\left(\chi_1\right)_i = 0$ and thus $\left(\Delta u^*\right)_i = \|\nabla u^*\|_{\mathcal{E}}^2$. We see that $\nu^S := \frac{u^*}{\|\nabla u^*\|_{\mathcal{E}}^2} \in \mathcal{V}_+$ is a solution of (M12).

To prove the final statement in M3, assume $\nu^S \in \mathcal{V}_+$ solves (M12). Then clearly $\operatorname{supp}(\nu^S) \subset S$. Assume there is a $j \in S$ such that $\nu_j^S = 0$, then (as in the proof of property M2 above) $(\Delta\nu^S)_j \le 0$. which contradicts (M12). Hence $S \subset \operatorname{supp}(u)$ and M3 is proven.

Note that by M2 we have that, for all $j \in V\setminus R$, $(\Delta\nu^R)_j \le \max_{i\in\operatorname{supp}(\nu^R)}(\Delta\nu^R)_i = 1$. To prove the statement in M4, we define $\tilde\nu := \nu^S - \nu^R$. Then $\tilde\nu = 0$ on $V\setminus S$, $\Delta\tilde\nu = 0$ on R and $\Delta\tilde\nu = 1 - \Delta\nu^R \ge 0$ on $S\setminus R$. Hence, by Lemma M3.1, we have that $\tilde\nu \ge 0$ on V.

10.2 Proof of Lemma M3.14

Remember the relation between G_{ij} and G_i^j from (M20) in the main paper.

We start with the Dirichlet case. Let $j \in S$. If $i \in V\setminus S$, then $\nu_i^S = \nu_i^{S\setminus\{j\}} = 0$, hence the boundary condition is satisfied. Next we note that, for $i \in S$,

$$\left(\Delta(\nu^S - \nu^{S\setminus\{j\}})\right)_i = \left(1 - (\Delta\nu^{S\setminus\{j\}})_j\right)\delta_{ij}. \tag{11}$$

Moreover,

$$\begin{aligned}\mathcal{M}(\nu^{S\setminus\{j\}}) &= \sum_{i\in S} d_i^r \nu_i^{S\setminus\{j\}} = \langle \Delta\nu^S, \nu^{S\setminus\{j\}}\rangle_{\mathcal{V}} \\ &= \langle \nu^S, \Delta\nu^{S\setminus\{j\}}\rangle_{\mathcal{V}} = \langle \nu^S, \chi_V\rangle_{\mathcal{V}} - \langle \nu^S, \chi_V - \Delta\nu^{S\setminus\{j\}}\rangle_{\mathcal{V}} \\ &= \mathcal{M}(\nu^S) - d_j^r\nu_j^S\left(1 - (\Delta\nu^{S\setminus\{j\}})_j\right).\end{aligned}$$

Hence $\frac{\nu_j^S}{\mathcal{M}(\nu^S)-\mathcal{M}(\nu^{S\setminus\{j\}})} = d_j^{-r}\left(1 - (\Delta\nu^{S\setminus\{j\}})_j\right)$, which, combined with (11), shows that, for all $i \in S$, $(\Delta G^j)_i = d_j^{-r}\delta_{ij}$. This proves the desired result in the Dirichlet case.

Next we consider the Poisson case. Since $\nu_k^{V\setminus\{k\}} = 0$, for all $j \in V$ the boundary condition $G_{k,j} = 0$ is satisfied.

Let $j \in V$. Using (M4), we compute $0 = \langle \Delta\nu^{V\setminus\{j\}}, \chi_V\rangle_{\mathcal{V}} = \sum_{i\in V\setminus\{j\}} d_i^r + d_j^r(\Delta\nu^{V\setminus\{j\}})_j$, hence, for all $i \in V$,

$$(\Delta\nu^{V\setminus\{j\}})_i = \begin{cases} 1, & \text{if } i \neq j, \\ -d_j^{-r}\mathrm{vol}\,(V\setminus\{j\}), & \text{if } i = j. \end{cases}$$

Note that

$$d_j^{-r}\mathrm{vol}\,(V\setminus\{j\}) = d_j^{-r}(\mathrm{vol}\,(V) - d_j^r) = d_j^{-r}\mathrm{vol}\,(V) - 1. \tag{12}$$

Since $\nu_k^{V\setminus\{j\}}$ is constant with respect to i, it does not contribute to ΔG^j. Hence we consider, for all $i \in V$,

$$\begin{aligned}\left(\Delta\left(\nu^{V\setminus\{k\}} - \nu^{V\setminus\{j\}}\right)\right)_i &= \left(1 + d_j^{-r}\mathrm{vol}\,(V\setminus\{j\})\right)\delta_{ij} - \left(1 + d_k^{-r}\mathrm{vol}\,(V\setminus\{k\})\right)\delta_{ik} \\ &= \mathrm{vol}\,(V)\,(d_j^{-r}\delta_{ij} - d_k^{-r}\delta_{ik}),\end{aligned}$$

where we used (12). This shows that, for all $i \in V$, $(\Delta G^j)_i = d_j^{-r}\delta_{ij} - d_k^{-r}\delta_{ik}$, which proves the result.

10.3 Proof of Lemma M5.17

First consider the case where z is constant, i.e. for all $l \in V$, $z_l = z_1$. Then, for any $w \in \mathcal{V}$ which satisfies the constraints in (M67), we have $\sum_{l\in V} w_l z_l = z_1 M$; hence any such w is trivially a minimizer. Moreover, the condition $z_i < z_j$ is never satisfied. Hence the result of the lemma holds. In the rest of the proof we assume z is not constant.

Next we note that, if $M = 0$, only $w = 0$ is admissible, in which case again the result of the lemma trivially holds. Hence we now assume $M > 0$.

Furthermore, if we define $\tilde{z} := z - z_n$, then, for all $l \in V$, $\tilde{z}_l \geq 0$. Moreover, for all $w \in \mathcal{V}$ which satisfy the constraints in (M67), we have $\sum_{l\in V} w_l z_l = \sum_{l\in V} w_l\tilde{z}_l + z_n\sum_{l\in V} w_l = \sum_{l\in V} w_l\tilde{z}_l + z_n M$. Hence we can assume, without loss of generality, that, for all $l \in V$, $z_l \geq 0$.

To prove the "only if" statement, let w^* be a minimizer for (M67) which satisfies the constraints. Assume for a proof by contradiction that there are $i, j \in V$ and $\varepsilon \in \left(0, \min(d_i^r, d_j^r)\right)$ such that $z_i < z_j$, $0 \leq w_i^* \leq d_i^r - \varepsilon$, and $\varepsilon \leq w_j^* \leq d_j^r$. Define $w^{**} \in \mathbb{R}^n$ by, for all $l \in V$,

$$w_l^{**} = \begin{cases} w_l^*, & \text{if } l \notin \{i, j\}, \\ w_i^* + \varepsilon, & \text{if } l = i, \\ w_j^* - \varepsilon, & \text{if } l = j. \end{cases}$$

Then $\sum_{l\in V} w_l^{**} = \sum_{l\in V} w_l^* = M$, for all $l \in V$, $0 \leq w_k^{**} \leq d_l^r$, and

$$\sum_{l\in V} w_l^{**} z_l = \sum_{l\in V} w_l^* z_l + \varepsilon(z_i - z_j) < \sum_{l\in V} w_l^* z_l.$$

This contradicts the fact that w^* is a minimizer. Hence, for all $i, j \in V$ and for all $\varepsilon \in \left(0, \min(d_i^r, d_j^r)\right)$, if $z_i < z_j$, then $w_i^* > d_i^r - \varepsilon$ or $w_j^* < \varepsilon$. Thus, if $z_i < z_j$, then $w_i^* = d_i^r$ or $w_j^* = 0$.

To prove the "if" statement in the lemma, assume that $w^* \in \mathcal{V}$ satisfies the constraints in (M67) and that for all $i, j \in V$, if $z_i < z_j$, then $w_i^* = d_i^r$ or $w_j^* = 0$. Let R^z be a relabelling function and let z^R and ${w^*}^R$ be the corresponding relabelled versions of z and w^*, respectively, as in (M66). For notational simplicity, we will drop the superscript R from z^R and ${w^*}^R$ in the rest of this proof. Define $L_1 := \min\{l \in V : w_l^* > 0\}$. Since $M > 0$, $w^* \neq 0$ and thus $L_1 \leq n$ exists.

Assume first that, for all $l > L_1$, $z_l = z_{L_1}$. Because, for all $l < L_1$, we have $w_l^* = 0$, we compute

$$\sum_{l\in V} w_l^* z_l = \sum_{l=L_1}^{n} w_l^* z_l = z_{L_1}\sum_{l=L_1}^{n} w_l^* = z_{L_1}\sum_{l\in V} w_l^* = z_{L_1} M.$$

Moreover we note that, by assumption $z_{L_1} = z_n = \min\{z_l \in \mathbb{R} : l \in V\}$, hence for all $w \in \mathcal{V}$ which satisfy the constraints in (M67), we have $\sum_{l\in V} w_l z_l \geq z_{L_1}\sum_{l\in V} = z_{L_1} M = \sum_{l\in V} w_l^* z_l$. Hence w^* is a minimizer in (M67).

Next we assume instead that there is an $l > L_1$, such that $z_l < z_{L_1}$. Define $L_2 := \min\{l \in V : z_l < z_{L_1}\}$ and let $w \in \mathcal{V}$ satisfy the constraints in (M67). Per definition $L_2 > L_1$. By construction we have that, for all $l \geq L_2$, $z_l < z_{L_1}$ and for all $l \in [L_1, L_2)$, $z_l = Z_{L_1}$. By definition $z_{L_1} \neq 0$, thus, by our assumption on w^* it follows that, for all $l \geq L_2$, $w_l^* = d_l^r \geq w_l$. We compute

$$\begin{aligned}\sum_{l=1}^{n} z_l w_l \geq \sum_{l=L_1}^{n} z_l w_l &= \sum_{l=L_1^n} (w_l^* - w_l)(z_{L_1} - z_l) - z_{L_1} \sum_{l=L_1}^{n} w_l^* + z_{L_1} \sum_{l=L_1}^{n} w_l + \sum_{l=L_1}^{n} w_l^* z_l \\ &= \sum_{l=L_2}^{n} (w_l^* - w_l)(z_{L_1} - z_l) - z_{L_1} M + z_{L_1} M + \sum_{l \in V} w_l^* z_l \geq \sum_{l \in V} w_l^* z_l.\end{aligned}$$

Hence also in this case w^* is a minimizer.

10.4 Direct computation of (8)

In this section we compute (8) using the eigenfunctions and eigenvalues as given in Lemma 6.8. For $j \in V$,

$$\varphi_i^j = \varphi_j^1 = 0 + \frac{1}{n}\left[(n-1)n\right]^{-1}(n-1)\left((n-1)\delta_{1j} - (1-\delta j1)\right) = \begin{cases} \frac{n-1}{n}, & \text{if } j = 1, \\ -\frac{1}{n^2}, & \text{if } j \neq 1. \end{cases}$$

Next we assume $i \neq 1 \neq j$. Let $I(k) := \{i \in \mathbb{N} : k \leq i \leq n\}$, for $k \in \mathbb{N}$. If $i = j$, we find

$$\begin{aligned}\varphi_i^i &= \sum_{m=1}^{n-2} \left[(n-m-1)^2 + (n-m-1)\right]^{-1} \left((n-m-1)\delta_{i,m+1} - \left(\chi_{I(m+2)}\right)_i\right)^2 \\ &\qquad + \frac{1}{n}\left[(n-1)n\right]^{-1} \\ &= \begin{cases} \frac{n-2}{n-1} + \frac{1}{n^2(n-1)}, & \text{if } i = 2, \\ \frac{n-i}{n-i+1} + \sum_{m=1}^{i-2} \frac{1}{(n-m-1)(n-m)} + \frac{1}{n^2(n-1)}, & \text{if } i \in \{3, \ldots, n-1\}, \\ \sum_{m=1}^{n-2} \frac{1}{(n-m-1)(n-m)} + \frac{1}{n^2(n-1)}, & \text{if } i = n, \end{cases} \\ &= \frac{n^2 - n - 1}{n^2}.\end{aligned}$$

The final equality above is not immediately obvious and follows from the fact that we have

$$\sum_{m=i-1}^{n-2} \frac{1}{(n-m-1)(n-m)} = \frac{n-i}{n-i+1}, \quad i \in \{3, \ldots, n-1\}, \tag{13}$$

$$\sum_{m=1}^{n-2} \frac{1}{(n-m-1)(n-m)} = \frac{n-2}{n-1}. \tag{14}$$

In Lemma 10.1 below we give a proof of the identities in (13), (14).

Finally, we consider the case $i \neq 1 \neq j \neq i$. Without loss of generality (because of symmetry under exchange of i and j) we assume that $i \leq j - 1$. Then

$$\begin{aligned}\varphi_i^j &= \sum_{m=1}^{n-2} \frac{\left((n-m-1)\delta_{i,m+1} - \left(\chi_{I(m+2)}\right)_i\right)\left((n-m-1)\delta_{j,m+1} - \left(\chi_{I(m+2)}\right)_j\right)}{(n-m-1)^2 + (n-m-1)} + \frac{1}{n^2(n-1)} \\ &= \begin{cases} -\frac{1}{n-1} + \frac{1}{n^2(n-1)}, & \text{if } i = 2, \\ \sum_{m-1}^{i-2} \frac{1}{(n-m-1)(n-m)} - \frac{1}{n-(i-1)} + \frac{1}{n^2(n-1)}, & \text{if } i \geq 3, \end{cases} \\ &= -\frac{n+1}{n^2},\end{aligned}$$

where for the last equality we have used that, for $i \geq 3$,

$$\sum_{m=1}^{i-2} \frac{1}{(n-m-1)(n-m)} = \frac{i-2}{(n-i+1)(n-1)}, \tag{15}$$

which is proven by subtracting (13) from (14). This completes the computation of (8). The following lemma shows that the identities in (13) and (14) hold.

Lemma 10.1. *For $N \in \mathbb{N}$, $N \geq 1$, we have*

$$\sum_{l=0}^{N-1} \frac{1}{(N-l)(N-l+1)} = \frac{N}{N+1}. \tag{16}$$

In particular, the identities in (13) and (14) hold.

Proof. First we prove (16) by induction. If $N = 1$ we immediately find that both the left and right hand side of (16) are equal to $\frac{1}{2}$. Now assume (16) is true for $N = k \in \mathbb{N}$, $k \geq 1$, then, for $N = k+1$ we compute

$$\begin{aligned}\sum_{l=0}^{k} \frac{1}{(k-l+1)(k-l+2)} &= \sum_{\tilde{l}=-1}^{k-1} \frac{1}{(k-\tilde{l})(k-\tilde{l}+1)} = \sum_{\tilde{l}=0}^{k-1} \frac{1}{(k-\tilde{l})(k-\tilde{l}+1)} + \frac{1}{(k+1)(k+2)} \\ &= \frac{k}{k+1} + \frac{1}{(k+1)(k+2)} = \frac{k+1}{k+2}.\end{aligned}$$

This proves (16). Setting $m = l + i - 1$ and $N = n - i$ proves (13). Setting $m = l + 1$ and $N = n - 2$ proves (14). □

The following corollary is used to prove (4).

Corollary 10.2. *Let $N, q \in \mathbb{N}$ such that $1 \leq q + 1 \leq N$. Then*

$$\sum_{l=2}^{q+1} \frac{1}{(N-l)(N-l+1)} = \frac{q}{(N-1)(N-q-1)}.$$

Proof. Using (15) we find

$$\sum_{l=2}^{q+1} \frac{1}{(N-l)(N-l+1)} = \sum_{l=1}^{q} \frac{1}{(N-l)(N-l-1)} = \frac{q}{(N-q-1)(N-1)}.$$

□

References

[AFP00] L. Ambrosio, N. Fusco, and D. Pallara, *Functions of bounded variation and free discontinuity problems*, first ed., Oxford Mathematical Monographs, Oxford University Press, Oxford, 2000.

[BCE03] ———, *Solving Dirichlet and Poisson problems on graphs by means of equilibrium measures*, European J. Combin. **24** (2003), no. 4, 365–375. MR 1975941 (2004f:05108)

[BF99] F. S. Bates and G. H. Fredrickson, *Block copolymers - designer soft materials*, Physics Today (February 1999), 32–38.

[BH09] T. Bühler and M. Hein, *Spectral clustering based on the graph p-laplacian*, Proceedings of the 26th Annual International Conference on Machine Learning, ACM, 2009, pp. 81–88.

[BPR14] D. P. Bourne, Mark A. Peletier, and S. M. Roper, *Hexagonal patterns in a simplified model for block copolymers*, SIAM Journal on Applied Mathematics **74** (2014), no. 5, 1315–1337.

[Bra02] Andrea Braides, Γ*-convergence for beginners*, first ed., Oxford Lecture Series in Mathematics and its Applications, vol. 22, Oxford University Press, Oxford, 2002.

[BV04] Stephen Boyd and Lieven Vandenberghe, *Convex optimization*, Cambridge university press, 2004.

[Cho12] Rustum Choksi, *On global minimizers for a variational problem with long-range interactions*, Quart. Appl. Math **70** (2012), 517–537.

[Chu97] Fan R. K. Chung, *Spectral graph theory*, CBMS Regional Conference Series in Mathematics, vol. 92, Published for the Conference Board of the Mathematical Sciences, Washington, DC, by the American Mathematical Society, Providence, Rhode Island, 1997. MR 1421568 (97k:58183)

[CMW11] Rustum Choksi, Mirjana Maras, and J. F. Williams, *2D phase diagram for minimizers of a Cahn-Hilliard functional with long-range interactions*, SIAM J. Appl. Dyn. Syst. **10** (2011), no. 4, 1344–1362. MR 2854591

[CP10] Rustum Choksi and Mark A Peletier, *Small volume fraction limit of the diblock copolymer problem: I. Sharp-interface functional*, SIAM Journal on Mathematical Analysis **42** (2010), no. 3, 1334–1370.

[CP11] ———, *Small volume-fraction limit of the diblock copolymer problem: II. Diffuse-interface functional*, SIAM Journal on Mathematical Analysis **43** (2011), no. 2, 739–763.

[CPW09] Rustum Choksi, Mark A. Peletier, and J. F. Williams, *On the phase diagram for microphase separation of diblock copolymers: an approach via a nonlocal Cahn-Hilliard functional*, SIAM J. Appl. Math. **69** (2009), no. 6, 1712–1738. MR 2496714

[CR03] R. Choksi and X. Ren, *On the derivation of a density functional theory for microphase separation of diblock copolymers*, Journal of Statistical Physics **113** (October 2003), no. 1/2, 151–176.

[CR05] ———, *Diblock copolymer/homopolymer blends: Derivation of a density functional theory*, Physica D **203** (2005), 100–119.

[CS06] R. Choksi and P. Sternberg, *On the first and second variations of a nonlocal isoperimetric problem*, J. reine angew. Math. **611** (2006), 75–108.

[DM93] G. Dal Maso, *An introduction to* Γ*-convergence*, first ed., Progress in Nonlinear Differential Equations and Their Applications, vol. 8, Birkhäuser, Boston, 1993.

[DS00] P. G. Doyle and J. L. Snell, *Random Walks and Electric Networks, Version 3.02*, ArXiv Mathematics e-prints math/0001057 (2000).

[Fie73] Miroslav Fiedler, *Algebraic connectivity of graphs*, Czechoslovak mathematical journal **23** (1973), no. 2, 298–305.

[GB06] A. Ghosh and S. Boyd, *Growing well-connected graphs*, Proceedings of the 45th IEEE Conference on Decision and Control, Dec 2006, pp. 6605–6611.

[GC09] Karl Glasner and Rustum Choksi, *Coarsening and self-organization in dilute diblock copolymer melts and mixtures*, Physica D: Nonlinear Phenomena **238** (2009), no. 14, 1241–1255.

[Giu84] E. Giusti, *Minimal surfaces and functions of bounded variation*, first ed., Monographs in Mathematics, vol. 80, Birkhäuser, Boston, 1984.

[Gla17] Karl Glasner, *Multilayered equilibria in a density functional model of copolymer-solvent mixtures*, SIAM Journal on Mathematical Analysis **49** (2017), no. 2, 1593–1620.

[Hal09] Jack K. Hale, *Ordinary differential equations*, second ed., Dover Publications, Inc., Mineola, New York, 2009.

[HJ90] Roger A. Horn and Charles R. Johnson, *Matrix analysis*, Cambridge University Press, Cambridge, 1990, Corrected reprint of the 1985 original. MR 1084815

[Ito98] Aya Ito, *Domain patterns in copolymer-homopolymer mixtures*, Physical Review E **58** (1998), no. 5, 6158.

[KOK88] K. Kawasaki, T. Ohta, and M. Kohrogui, *Equilibrium morpholoy of block copolymer melts. 2*, Macromolecules **21** (1988), 2972–2980.

[Le10] Nam Q. Le, *On the convergence of the Ohta–Kawasaki equation to motion by nonlocal Mullins–Sekerka law*, SIAM Journal on Mathematical Analysis **42** (2010), no. 4, 1602–1638.

[MM77] Luciano Modica and Stefano Mortola, *Un esempio di Γ^--convergenza*, Bollettino U.M.I. **5** (1977), no. 14-B, 285–299.

[Mod87a] Luciano Modica, *The gradient theory of phase transitions and the minimal interface criterion*, Arch. Rational Mech. Anal. **98** (1987), no. 2, 123–142. MR 866718 (88f:76038)

[Mod87b] ———, *Gradient theory of phase transitions with boundary contact energy*, Ann. Inst. Henri Poincaré **4** (1987), no. 5, 487–512.

[New] *Network data — Mark Newman*, http://www-personal.umich.edu/~mejn/netdata/, last accessed: 28 August, 2017.

[NW99] Jorge Nocedal and Stephen J. Wright, *Numerical optimization*, Springer Series in Operations Research, Springer-Verlag, New York, 1999. MR 1713114 (2001b:90002)

[OBO13] Braxton Osting, Christoph Brune, and Stanley Osher, *Enhanced statistical rankings via targeted data collection*, Proceedings of the 30th International Conference on Machine Learning (Atlanta, Georgia, USA) (Sanjoy Dasgupta and David McAllester, eds.), vol. 28, Proceedings of Machine Learning Research, no. 1, PMLR, 17–19 Jun 2013, pp. 489–497.

[OBO14] Braxton Osting, Christoph Brune, and Stanley J Osher, *Optimal data collection for informative rankings expose well-connected graphs*, Journal of machine learning research **15** (2014), 2981–3012.

[OK86] T. Ohta and K. Kawasaki, *Equilibrium morpholoy of block copolymer melts*, Macromolecules **19** (1986), 2621–2632.

[PV10] Mark A Peletier and Marco Veneroni, *Stripe patterns in a model for block copolymers*, Mathematical Models and Methods in Applied Sciences **20** (2010), no. 06, 843–907.

[RS] Michael Reed and Barry Simon, *Methods of modern mathematical physics i: Functional analysis.*

[RW00] X. Ren and J. Wei, *On the multiplicity of solutions of two nonlocal variational problems*, SIAM J. Math. Anal. **31** (2000), no. 4, 909–924.

[RW02] ———, *Concentrically layered energy equilibria of the diblock copolymer problem*, Euro. Jnl of Applied Mathematics **13** (2002), 479–496.

[RW03a] ———, *On energy minimizers of the di-block copolymer problem*, Interfaces Free Boundaries **5** (2003), no. 2, 193–238.

[RW03b] ———, *On the spectra of three-dimensional lamellar solutions of the diblock copolymer problem*, SIAM J. Math. Anal. **35** (2003), no. 1, 1–32.

[RW14] Xiaofeng Ren and Juncheng Wei, *Double tori solution to an equation of mean curvature and newtonian potential*, Calculus of Variations and Partial Differential Equations **49** (2014), no. 3-4, 987–1018.

[RW17] ———, *The spectrum of the torus profile to a geometric variational problem with long range interaction*, Physica D: Nonlinear Phenomena (2017).

[Sig] Karl Sigman, *Lecture notes on stochastic modelling i*, http://www.columbia.edu/~ks20/stochastic-I/stochastic-I.html.

[UD05] T. Uneyama and M. Doi, *Density functional theory for block copolymer melts and blends*, Macromolecules **38** (2005), 196–205.

[vG] Yves van Gennip, *Extensions and corrections for "Mean curvature, threshold dynamics, and phase field theory on finite graphs"*, in prep.

[vG08] Y. van Gennip, *Partial localisation in a variational model for diblock copolymer-homopolymer blends*, Ph.D. Thesis Technische Universiteit Eindhoven, 2008, ISBN 978-90-386-1404-5, http://alexandria.tue.nl/extra2/200811534.pdf.

[vGB12] Y. van Gennip and A. L. Bertozzi, Γ*-convergence of graph Ginzburg-Landau functionals*, Adv. Differential Equations **17** (2012), no. 11–12, 1115–1180.

[vGGOB14] Y. van Gennip, N. Guillen, B. Osting, and A. L. Bertozzi, *Mean curvature, threshold dynamics, and phase field theory on finite graphs*, Milan Journal of Mathematics **82** (2014), no. 1, 3–65.

[vGP08] Yves van Gennip and Mark A. Peletier, *Copolymer-homopolymer blends: global energy minimisation and global energy bounds*, Calc. Var. Partial Differential Equations **33** (2008), no. 1, 75–111.

[vGP09] ———, *Stability of monolayers and bilayers in a copolymer-homopolymer blend model*, Interfaces Free Bound. **11** (2009), no. 3, 331–373.

[vGP11] ———, *The H^{-1}-norm of tubular neighbourhoods of curves*, ESAIM Control Optim. Calc. Var. **17** (2011), no. 1, 131–154. MR 2775190 (2012c:49025)

[WS98] D. J. Watts and S. H. Strogatz, *Collective dynamics of 'small-world' networks.*, Nature **393** (1998), no. 6684, 440–442.

[WSTB86] John G White, Eileen Southgate, J Nichol Thomson, and Sydney Brenner, *The structure of the nervous system of the nematode caenorhabditis elegans: the mind of a worm*, Phil. Trans. R. Soc. Lond **314** (1986), 1–340.